

MOL #21741

Caveolin-1 Regulates Store-Operated Ca²⁺ Influx by Binding of its Scaffolding Domain to TRPC1 in Endothelial Cells

Angela M. Kwiatek, Richard D. Minshall, David R. Cool, Randal A. Skidgel, Asrar B. Malik,
and Chinnaswamy Tiruppathi.

AMK, RDM, RAS, ABM, CT: Department of Pharmacology and Center for Lung and Vascular Biology, College of Medicine, University of Illinois at Chicago, Chicago, IL 60612.

DRC: Department of Pharmacology/Toxicology, Boonshoft School of Medicine, Wright State University, Dayton, OH 45435.

Running Title: Caveolin-1 regulates store-operated Ca^{2+} influx

Address for correspondence: Chinnaswamy Tiruppathi, Ph.D.
Department of Pharmacology (M/C868)
College of Medicine
University of Illinois at Chicago
835 S. Wolcott Ave, Chicago, IL 60612
Phone: (312) 355-0249
Fax: (312) 996-1225
E-mail: tiruc@uic.edu

Text Pages: 34

Table: 1

Figures: 5

References: 40

Abstract: 185 words;

Introduction: 717 words

Discussion: 1014 words

Abbreviations: SOCs, store-operated cation channels; TRPC1, transient receptor potential channel-1; CSD, caveolin-1 scaffolding domain; HPAEC, human pulmonary artery endothelial cells.

Abstract:

Caveolin-1 associates with store-operated cation channels (SOC) in endothelial cells. We examined the role of the caveolin-1 scaffolding domain (CSD) in regulating the SOC (i.e., transient receptor potential channel-1 [TRPC1]) in human pulmonary artery endothelial cells (HPAEC). We used the cell permeant antennapedia (AP)-conjugated CSD peptide, which competes for protein binding partners with caveolin-1, to assess the interactions of caveolin-1 with TRPC1 and its consequences on thrombin-induced Ca^{2+} influx. We observed that AP-CSD peptide markedly reduced thrombin-induced Ca^{2+} influx via SOC in HPAEC in contrast to control peptide. AP-CSD also suppressed thapsigargin-induced Ca^{2+} influx. Streptavidin-bead pull-down assay indicated strong binding of biotin-labeled AP-CSD peptide to TRPC1. Immunoprecipitation studies demonstrated an interaction between endogenous TRPC1 and ectopically expressed HA-tagged-CSD. Analysis of the deduced TRPC1 amino acid sequence revealed the presence of CSD binding consensus sequence in the TRPC1-C-terminus. We also observed that an AP-TRPC1 peptide containing the CSD binding sequence markedly reduced the thrombin-induced Ca^{2+} influx. We identified the interaction between biotin-labeled AP-TRPC1 C-terminus peptide and caveolin-1. Thus, these results demonstrate a crucial role of caveolin-1 scaffolding domain interaction with TRPC1 in regulating Ca^{2+} influx via SOC.

Pro-inflammatory mediators such as thrombin, histamine, and reactive oxygen species increase vascular permeability in part by activating Ca^{2+} -sensitive signaling pathways (Tiruppathi et al., 2003). We showed that Ca^{2+} entry through plasma membrane cation channels activated by Ca^{2+} store depletion is a critical determinant of increased endothelial permeability (Sandoval et al., 2001a; Sandoval et al., 2001b; Tiruppathi et al., 2002). We have also shown that activation of endothelial cell surface protease-activated receptor-1 (PAR-1) by thrombin caused a rapid and transient increase in cytosolic Ca^{2+} concentration ($[\text{Ca}^{2+}]_i$) due to the release of stored Ca^{2+} and subsequent Ca^{2+} entry induced by store depletion (Sandoval et al., 2001a). In endothelial cells, the plasma membrane cation channels known as store-operated cation channels (SOCs) contribute to the entry of Ca^{2+} into cells (Nilius and Droogmans, 2001). Several studies have shown the important role the influx of Ca^{2+} through SOCs in vascular endothelial cells (Tiruppathi et al., 2002; Nilius and Droogmans, 2001; Freichel et al., 2001). Studies identified that the mammalian homologues of transient receptor potential (TRP) gene family of channels function as SOCs (Nilius and Droogmans, 2001; Tiruppathi et al., 2003). TRP genes encode a superfamily of proteins with 6 transmembrane helices that are divided into 7 subfamilies: TRPC (Canonical or Classical), TRPV (Vanilloid), TRPM (Melastatin), TRPA (Ankyrin), TRPML (Mucolipin), TRPP (Polycystin), and the TRPN (no mechanoreceptor potential C [NOMPC]) (Pedersen et al., 2005; Montell et al., 2002). Members of TRPC subfamily contain 700 to 1000 amino acids and 7 isoforms (TRPC1 to 7) that are expressed in mammalian cells. Mammalian TRPCs are grouped into 4 subfamilies. i) One group consists of TRPC4 and TRPC5. Their activation is dependent on Ca^{2+} -store depletion and they have high Ca^{2+} selectivity as assessed by their sensitivity to La^{3+} (Nilius and Droogmans, 2001). TRPC4 and TRPC5 are activated by G protein-coupled receptors and receptor tyrosine kinases coupled to phospholipase C (PLC). ii)

TRPC1 is closely related to TRPC4 and TRPC5; although it forms SOCs, it is a less selective Ca^{2+} channel. iii) TRPC3, TRPC6, and TRPC7 form store-independent non-selective cation channels activated by diacylglycerol (DAG) (Dietrich et al, 2003); however, a store-dependent activation mechanism has been described for human TRPC3 (Liu et al., 2000). iv) TRPC2 function is unclear and it is believed to be a pseudogene in humans (Montell et al., 2002).

TRPC1 has been shown to be localized within cholesterol-rich invaginations of the cell membrane called caveolae (Brazer et al., 2003). Caveolae are coated with a 22 kDa protein, caveolin-1 (Cav-1). Studies have shown that Ca^{2+} influx occurs via caveolae in response to ER store Ca^{2+} depletion in endothelial cells (Isshiki et al., 2002). Further, Cav-1 appears to be necessary for anchoring TRPC1 to caveolae (Lockwich et al., 2000), but it is unclear how this interaction regulates TRPC1 function in endothelial cells. Cav-1 scaffolding domain (CSD), located between residues 82 and 101 of Cav-1, binds many signaling molecules including endothelial nitric oxide synthase (eNOS), *Src*-like kinases, Ha-Ras, and heterotrimeric G-proteins (Schlegel and Listanti, 2001). Binding of these proteins to CSD in many cases negatively regulates their function (Drab et al., 2001). For example, binding of eNOS to CSD, holds eNOS in an inactive state. Bucci et al (2000) observed inhibition of acetylcholine-induced NO production and vasodilation in bovine aortic endothelial cells by cell membrane permeable CSD-peptide. Moreover, acute vascular inflammation in mice was prevented by systemic administration of cell-permeable CSD-peptide. Another study demonstrated that CSD-peptide administration markedly reduced platelet-activating factor-induced increase in microvessel permeability in rats (Zhu et al, 2004). Recently Bernatchez et al (2005) have shown that CSD sequence containing the residues 89-95 is sufficient to inhibit eNOS activity and NO release from endothelial cells. Since Ca^{2+} signaling in the endothelium is critical in regulating

endothelial permeability, we addressed the possible role of CSD in the TRPC1-mediated Ca^{2+} influx in endothelial cells. We observed that cell-permeable CSD-sequence markedly reduced ER store Ca^{2+} release and the Ca^{2+} release-activated Ca^{2+} influx in response to thrombin challenge of endothelial cells. This response was dependent on the specific interaction between CSD and TRPC1. Analysis of the deduced TRPC1 amino acid sequence revealed the presence of CSD binding consensus sequence in TRPC1-C-terminus. A synthetic peptide corresponding to CSD binding consensus sequence present in the C-terminus of TRPC1 was shown to inhibit the thrombin-induced Ca^{2+} influx in endothelial cells.

Materials and Methods

Materials

Human α -thrombin was obtained from Enzyme Research Laboratories (South Bend, IN). Endothelial growth medium (EGM-2) was obtained from Cambrex Bio Science (Walkersville, MD). Hanks' balanced salt solution (HBSS) and trypsin were from Invitrogen, (Carlsbad, CA). Fetal bovine serum (FBS) was from HyClone (Logan, UT). Fura 2-AM was purchased from Molecular Probes (Eugene, OR). Anti-HA monoclonal antibody (mAb) was obtained from Sigma (St. Louis, MO). Anti-*cSrc* monoclonal and anti-TRPC1 polyclonal antibodies were obtained from Santa Cruz Biotechnology (Santa Cruz, CA). Streptavidin cross-linked agarose and Streptavidin conjugated rhodamine were obtained from Pierce Biotechnology (Rockford, IL). Peptides were synthesized at commercial facility (bioWORLD, Dublin, OH). Cav-1 scaffolding domain (CSD) sequence (amino acids 82-101, DGIWKASFTTFTVTKYWFYR) was synthesized as a fusion peptide to the C terminus of the antennapedia (AP) internalization sequence (RQIKIWFQNRRMKWKK) (Bucci et al., 2000). The cell permeable antennapedia (AP) sequence was used as a control peptide. The C-terminal TRPC1 peptide (amino acids 781-789 [FRTSKYAMF]) was synthesized as a fusion peptide to the C terminus of the AP internalization sequence. All peptides were synthesized as C-terminal amide and N-terminus was labeled with biotin. Peptides purity and amino acid sequence were determined by HPLC and MS, respectively. Peptides used in this study were 98% pure.

Cell culture

Human pulmonary artery endothelial cells (HPAEC) were grown in EGM-2 medium supplemented with 10% FBS. Cells were cultured on tissue culture dishes coated with 0.1%

gelatin. HPAEC used in the experiments were between 5 and 7 passages. Human dermal microvessel endothelial cell line (HMEC) was grown as described (Ellis et al., 1999).

Cell volume measurement

HPAEC grown in 100 mm culture dishes were incubated with 1% FBS medium in the presence of 1 $\mu\text{Ci/ml}$ [^3H]-D-Mannitol (D-[1- ^3H (N)]-mannitol) for 4 h at 37°C to reach equilibrium. After incubation, cells were placed on ice and washed 2X with HBSS. Cells were lysed with lysis buffer (50 mM Tris-HCl buffer pH 7.4, containing 0.5% sodium deoxycholate, 1% Triton X-100) for 1 h at 4°C. The radioactivity associated with the cell lysate was determined using liquid scintillation counter. HPAEC grown in culture dishes were trypsinized and cell numbers were counted. Cell volume was determined using the equilibrium [^3H]-D-Mannitol uptake and cell numbers. Based on these measurements, we obtained cell volume of 2.5 $\mu\text{l}/10^6$ cells.

Measurement of peptide concentration inside HPAEC

Cell permeable peptides reached inside HPAEC were determined using surface enhanced laser/desorption ionization-time of flight mass spectrometry (SELDI-TOF MS) as described previously (Cool and Hardiman, 2004; Hardiman et al., 2005). HPAEC grown to confluence on 100 mm culture dishes were incubated with 1% FBS containing medium in the presence or absence of the AP or AP-CSD peptide for 4 h at 37°C. After the incubation, cells were placed on ice and washed 2X with acid buffer (50 mM acetate buffer pH 4.5 containing 0.15 M NaCl). Then cells were washed 2X with HBSS, scraped, and pelleted by centrifugation at 500xg for 10 min. The cell pellet (contain $\sim 1.6 \times 10^6$ cells) was homogenized in 20 μl 0.1 N HCl and centrifuged for 5 min at 13,000 rpm to remove cell debris. The supernatant was applied on the CiphergenWCX2 (weak cation exchange) ProteinChip[®]. The sample spots were allowed to

nearly dry (still damp), then rinsed individually with 5 μ l of water to remove unwanted and unbound debris. The EAM (energy absorbing molecule) matrix (1 μ l), alpha-cyano-4-hydroxy cinnamic acid (CHCA), in 50% acetonitrile and 0.1% TFA, was added to each spot to aide in the ionization of peptides. The ProteinChips[®] were placed into the CIPHERGEN SELDI-TOF ProteinChip[®] Array for analysis. A spot and chip protocol were designed to take 10 transients at every five sites beginning at 20 and ending at 80 (each spot has 100 possible sites). The laser intensity was set to 155 for each sample with two warming shots at 160 intensity. The CIPHERGEN v3.2 software was used to analyze each spectra for the peptides of choice. The CSD and AP peptides were suspended in 0.1 N HCl to a concentration of 1 mM and serial 1:5 dilutions were analyzed for both peptides. Integrated area under each observed ion peak was plotted against the concentration of peptide and the linear regression formula determined. The concentrations of the peptides in the cell lysate samples were determined using this formula.

Cytosolic Ca²⁺ measurement

Increase in cytosolic Ca²⁺ ([Ca²⁺]_i) was measured using the Ca²⁺-sensitive fluorescent dye Fura2-AM (Tiruppathi et al., 2002). Cells were grown to confluence on 0.1% gelatin-coated 25 mm glass cover slips to confluence. Cells were incubated with or without peptides in 1% FBS containing medium for 4 h at 37°C. Cells were washed 2X with HBSS and loaded with 3 μ M Fura2-AM for 30 min. Cells were washed again 2X with HBSS and then imaged using an Attoflor Ratio Vision digital fluorescence microscopy system (Atto Instruments) equipped with a Zeiss Axiovert S 100 inverted microscope and F-Fluar 40x, 1.3 NA oil immersion objective. Regions of interest in individual cells were marked and excited at 334 and 380 nm with emission at 520 nm at 5-second intervals. In each experiment, 30 to 50 cells were selected to measure change in [Ca²⁺]_i. The cells were then stimulated with either thrombin or thapsigargin. The area

under the curve (the total Ca^{2+} transient peak, ER store Ca^{2+} release peak, and influx peak) were quantified using ImageJ 1.31v Program.

Streptavidin-agarose beads affinity precipitation

Proteins bound to biotin labeled peptides were precipitated using streptavidin-agarose beads. HPAEC grown to confluence were incubated with either AP-CSD or AP at the indicated concentration for 4 h at 37°C. After incubation, cells were placed on ice and washed 2X with HBSS. Cells were lysed with lysis buffer (50mM Tris-HCl buffer pH 7.4, containing 0.5% sodium deoxycholate, 1% Triton X-100, 1 mM orthovanadate, protease inhibitors) for 1 h at 4°C. The lysates were centrifuged at 60,000xg for 30 min. The obtained supernatant was mixed with streptavidin-agarose beads and incubated for 1 h at 4°C with shaking. After this treatment, the suspension was centrifuged at 5000xg for 10 min. The supernatant was discarded, and the beads were washed 3X with 50mM Tris-HCl buffer pH 7.4, containing 1 M NaCl and 0.1% Triton X-100. After removing the supernatant from the last wash, SDS-PAGE sample buffer was added to the beads, boiled for 5 min, and centrifuged at 5000xg for 5 min at 22°C. Proteins present in the supernatant were separated on an SDS-PAGE and immunoblotted with the appropriate antibodies.

Preparation of expression constructs

Myc-TRPC1 cDNA expression construct was prepared as described (Paria et al., 2003). Caveolin-1 wild type (Wt-Cav-1) cDNA in pcDNA3.1 expression construct was made as described (Minshall et al., 2000). Cav-1-14F mutant was prepared by PCR method using the QuickChange Site Directed Mutagenesis Kit (Stratagene). HA-tagged caveolin-1 scaffolding domain (CSD) expression construct was also prepared using PCR method. To generate N-terminal HA-tagged CSD domain, the human wild type Cav-1 was PCR amplified using the

following primers: forward, 5'-ACAGAATTCGCACACGGCATTTGGAAG-3', and reverse, 5'-ACAACACTCGAGTTATTAGCGGTAAAACCAG-3'. The resulting DNA fragment (63 bp) was subcloned into the 5'-*EcoRI* and 3'-*XhoI* restriction sites (underlined in primers) of pcDNA3-HA vector. Cav-1-14F mutant and HA-tagged CSD expression constructs sequences were verified by DNA sequencing. These expression constructs were transfected into HMEC using LipofectAMINE Plus reagent in serum free Dulbecco's modified Eagle's medium as we described (Ellis et al., 1999). At 48 h after transfection, cells were used for intracellular Ca²⁺ measurement and immunoprecipitation experiments.

Statistics

Statistical comparisons were made using the two-tailed Student's *t* test. Experimental values were reported as means \pm S.E. Differences in mean values were considered significant at $p < 0.05$.

Results

Cell permeable Cav-1 Scaffolding Domain (CSD) Peptide Inhibits Thrombin-Induced Increase in $[Ca^{2+}]_i$

We determined the contribution of Cav-1 scaffolding domain (CSD) in regulating the thrombin-induced increase in $[Ca^{2+}]_i$ in HPAEC. We synthesized the CSD sequence (residues 82-101, DGIWKASFTTFTVTKYWFYR) as a fusion peptide to the C terminus of antennapedia (AP) internalization sequence (RQIKIWFQNRRMKWKK) (Bucci et al., 2000). Cell-permeable AP peptide was used as control as described (Bernatchez et al., 2005; Zhu et al., 2004). The peptides were biotinylated at the N-terminus to detect their internalization in endothelial cells. We observed the internalization of both AP-CSD and AP in HPAEC by staining with rhodamine-labeled streptavidin (**Fig. 1A**). We also determined the relative concentration of the peptides reached inside HPAEC utilizing SELDI-TOF MS (**Fig. 1B and Table 1**, see details in **Methods**). We observed the presence of 25 μ M and 80 μ M of AP peptide by incubating cells with 50 μ M and 100 μ M concentrations respectively in the extracellular medium for 4 h (Table 1). In the case of AP-CSD peptide, we observed the presence of 20 μ M and 65 μ M inside the cells by incubating cells with 50 μ M and 100 μ M concentrations respectively in the extracellular medium (**Table 1**). These results indicate the presence of both the AP and AP-CSD peptides inside the HPAEC. Next, we determined the effects of AP-CSD and AP on thrombin-induced increase in $[Ca^{2+}]_i$. Thrombin-induced increase in $[Ca^{2+}]_i$ was inhibited in cells incubated with AP-CSD in a dose-dependent manner compared with control cells (**Fig. 1C**); however, control AP had no significant effect on thrombin-induced increase in $[Ca^{2+}]_i$ (**Fig. 1D**). To address whether AP-CSD peptide inhibits thrombin-induced Ca^{2+} influx, HPAEC incubated with AP-CSD peptide were first stimulated with thrombin in the absence of extracellular Ca^{2+} , and then

Ca^{2+} was added to the extracellular medium to assess Ca^{2+} influx. We observed that in the absence of extracellular Ca^{2+} , thrombin-induced increase in initial peak due to ER store Ca^{2+} depletion was markedly reduced in AP-CSD-treated cells compared to control (**Fig. 2A and B**), whereas AP alone did not influence the initial peak (data not shown). Ca^{2+} influx after ER store Ca^{2+} depletion induced by thrombin was also significantly reduced in HPAEC exposed to AP-CSD compared to control (**Fig. 2A and B**). These results demonstrate that CSD regulates both IP_3 -sensitive ER store Ca^{2+} depletion and store Ca^{2+} depletion-mediated Ca^{2+} influx in endothelial cells.

To characterize further the basis of inhibition of Ca^{2+} influx by the AP-CSD in HPAEC, we measured the thapsigargin-induced increase in intracellular Ca^{2+} in AP-CSD or AP treated HPAEC. Thapsigargin-induced increase in intracellular Ca^{2+} was also markedly reduced in AP-CSD incubated cells compared to AP or control cells (**Fig. 2C**), suggesting that CSD interacts with TRPC1 to prevent Ca^{2+} influx in HPAEC.

CSD interacts with TRPC1 in endothelial cells

We have shown that TRPC1 is predominantly expressed in human vascular endothelial cells (Paria et al., 2003; Paria et al., 2004; Paria et al., 2006). Other studies have shown that assembly of TRPC1 in a signaling complex associated with Cav-1 (Lockwich et al., 2000) and this association was necessary for SOC-mediated Ca^{2+} influx (Brazer et al., 2003). However, it is unclear whether CSD directly interacts with TRPC1 and whether this interaction is necessary for SOC-mediated Ca^{2+} influx in endothelial cells. To address this question, we incubated AP-CSD or AP with HPAEC for 4 h at 37°C, cells were washed 3 times with acid buffer to remove surface bound peptides, and cells were lysed. Lysates were incubated with streptavidin-agarose-beads to study the binding of TRPC1 with AP-CSD (see details in **Methods**). Streptavidin-

agarose beads were washed and bound proteins were separated on SDS-PAGE, and immunoblotted with anti-TRPC1 Ab (**Fig. 3A**). Anti-TRPC1 Ab strongly reacted with ~85 kDa protein (TRPC1) in AP-CSD treated cells, whereas there was a weak reaction of anti-TRPC1 Ab with TRPC1 in AP peptide-incubated cells.

To address the specificity of the interaction between CSD and TRPC1, we ectopically expressed HA-tagged-CSD in HMEC and at 48 h after transfection, cells were lysed and lysates were immunoprecipitated with anti-HA antibody. The precipitated proteins were immunoblotted with anti-TRPC1 Ab (**Fig. 3B**). We observed that anti-TRPC1 Ab reaction with TRPC1 only in cell lysate from HA-tagged-CSD transfected cells but not in vector alone transfected cells. These results indicate interaction between TRPC1 and CSD in endothelial cells.

CSD interacts with C-terminus of TRPC1

Previous studies have shown that binding of CSD to aromatic amino acids containing motifs: $\Phi X \Phi X X X X \Phi$ and $\Phi X X X X \Phi X X \Phi$, where Φ is an aromatic residue (Trp, Phe, or Tyr) (Couet et al., 1997). The deduced amino acid sequence of TRPC1 revealed the presence of a similar CSD binding motif in the C-terminus (FRTSKYAMF [$\Phi X X X X \Phi X X \Phi$]). To study the interaction between TRPC1 C-terminal peptide with CSD, we synthesized TRPC1 C-terminal peptide (residues 781-789; FRTSKYAMF [**Fig. 4A**]) as cell permeable AP fusion peptide with biotin at the N-terminus (AP-TRPC1-C9) (see details in **Methods**). HPAEC were incubated with AP-TRPC1-C9 for 4 h, cells were washed, lysed, and lysates were incubated with streptavidin-agarose beads (see details in **Methods**). Proteins associated with streptavidin-agarose beads were separated on SDS-PAGE and immunoblotted with anti-Cav-1 Ab. We observed that the anti-Cav-1 Ab reacted with Cav-1 present in streptavidin-agarose precipitated proteins from TRPC1 C-terminal peptide incubated cells (**Fig. 4B**), but not from the AP sequence-incubated

cells, indicating that TRPC1 C-terminal sequence (FRTSKYAMF) interacts with Cav-1 in endothelial cells.

TRPC1 C-terminal peptide inhibits thrombin-induced increase in intracellular Ca^{2+} in HPAEC

We next examined the effects of cell permeable TRPC1 C-terminal peptide on thrombin-induced increase in $[Ca^{2+}]_i$ in HPAEC. We observed that AP-TRPC1-C9 peptide pretreatment inhibited in a dose-dependent manner the thrombin-induced increase in $[Ca^{2+}]_i$ in HPAEC (**Fig. 4C and D**). We also tested the effects of AP-TRPC1-C9 peptide on ER store Ca^{2+} release and Ca^{2+} release activated Ca^{2+} influx in HPAEC. In this experiment, after Fura-2 AM loading, cells were stimulated with thrombin in the absence of extracellular Ca^{2+} to deplete ER stored Ca^{2+} , and then Ca^{2+} was reapplied to assess the Ca^{2+} influx. AP-TRPC1-C9 peptide had significant effect on Ca^{2+} release from ER (**Fig. 4E and F**). Also, AP-TRPC1-C9 peptide exposure markedly reduced the Ca^{2+} influx induced by thrombin (**Fig. 4E and F**), suggesting that TRPC1-C9 peptide competes for the CSD binding domain on TRPC1.

CSD peptide binds to Src and inhibits Cav-1-Tyr14 phosphorylation in endothelial cells

Studies have shown that CSD interacts with signaling molecules such as *Src* and phosphorylates Cav-1 on Tyr-14 (Minshall et al., 2000; Oh and Schnitzer, 2001, Schlegel and Lisanti, 2001; del Pozo et al., 2005); thus, we determined whether AP-CSD also interacts with *Src* in HPAEC. HPAEC were incubated the biotin labeled AP-CSD or AP for 4 h and cell lysates were used for streptavidin-agarose bead pull-down assays (see details in **Methods**). We observed binding of *Src* with AP-CSD peptide but not with AP-peptide (**Fig. 5A**), indicating that CSD interacts with *Src* and thus may regulate SOC function in HPAEC by this mechanism.

Studies have shown that *Src*-mediated Cav-1 phosphorylation on Tyr-14 is crucial in signal transduction events in caveolae (del Pozo et al., 2005; Shajahan et al., 2004); thus, we determined the possibility that CSD peptide inhibits Cav-1 phosphorylation on Tyr-14 in HPAEC and interferes with SOC-mediated Ca^{2+} influx. HPAEC were incubated with either AP-CSD or AP and challenged with thrombin, and cell lysates were immunoblotted with anti-phospho-Tyr-14 Cav-1 specific antibody. In control cells (i.e., in absence of thrombin-stimulation), we observed Cav-1 phosphorylation on Tyr-14; however, phosphorylation was further increased on thrombin stimulation. Maximum phosphorylation was seen at 2 min after thrombin challenge, and it returned to baseline at 10 min (**Fig. 5B**). Treatment of cells with AP-CSD at a concentration less than 25 μM prevented both basal and thrombin-induced Tyr-14 phosphorylation of Cav-1 whereas the control peptide (AP-peptide) had no effect (**Fig. 5B**).

Co-expression of Cav-1 and TRPC1 inhibits thrombin-induced increase in $[\text{Ca}^{2+}]_i$ in endothelial cells

We have shown that increased SOC-mediated Ca^{2+} influx occurs in TRPC1 over-expressing endothelial cells (Paria et al., 2004); thus, we investigated the effects of Cav-1 over-expression on TRPC1-mediated Ca^{2+} influx in endothelial cells. We ectopically expressed Myc-TRPC1, Myc-TRPC1 plus WT-Cav-1, or Myc-TRPC1 plus Cav-1-14F mutant in HMEC. Expression levels of Myc-TRPC1, WT-Cav-1, and Cav-1-14F mutant were determined by immunoblotting transfected HMEC lysates with anti-Myc mAb and anti-Cav-1 Ab (**Fig. 5C**). Thrombin produced a 2-fold increase in $[\text{Ca}^{2+}]_i$ in Myc-TRPC1 expressing HMEC compared to control (vector alone transfected) cells (**Fig. 5D and 5E**). Co-expression of WT-Cav-1 with Myc-TRPC1 reduced the thrombin-induced increase in $[\text{Ca}^{2+}]_i$ in HMEC. Also, co-expression of phosphorylation-defective Cav-1 mutant (Cav-1-14F) with Myc-TRPC1 resulted in the same

MOL #21741

reduction in thrombin-induced increase in $[Ca^{2+}]_i$. Thus, Cav-1 may regulate SOC function by directly binding to TRPC1 and Cav-1 phosphorylation on Tyr-14 does not appear to be required for Ca^{2+} entry via SOC.

Discussion

Ca²⁺ entry in non-excitabile cells via store-operated cation channels (SOCs) regulates many signaling events including gene expression, cell survival, and cell death (Nilius and Droogmans, 2001; Birnbaumer et al., 2003; Montell et al., 2002; Putney, 1999). We have shown that Ca²⁺ entry via SOC in endothelial cells is crucial in regulating vessel wall barrier function (Tiruppathi et al., 2003). Our studies (Paria et al., 2003; Paria et al., 2004; Paria et al., 2006) and others (Groschner et al., 1998; Broough et al., 2001) have demonstrated that TRPC1 expressed in human vascular endothelial cells is an essential component of SOC. TRPC1 can be activated by the G_{αq/11}-linked phospholipase C pathway (Tiruppathi et al., 2003; Nilius and Droogmans, 2001). However, the molecular mechanism of Ca²⁺ influx through TRPC1 is not well understood. Brazer et al (2003) showed the specific binding of Cav-1 with N- and C-termini of TRPC1 in human submandibular gland cells. They also showed that interaction between Cav-1 and TRPC1 was essential for the membrane localization of TRPC1 and that Cav-1 N-terminus domain (residues 51-169) binding to TRPC1 was involved in regulating Ca²⁺ influx through TRPC1. However, it is known that Cav-1 N-terminus contains a scaffolding domain (i.e., residues 82-101 [CSD]), which regulates key signaling events. For example, binding of eNOS to CSD prevented NOS activation in endothelial cells (Bucci et al., 2000). Also, Ca²⁺ influx through SOC was shown to disrupt the eNOS interaction with CSD, and thus facilitated the binding of eNOS to Ca²⁺/calmodulin complex required for activation eNOS (Michel et al., 1997). Since CSD is localized in the N-terminus of Cav-1, in the present study we addressed the possible role of CSD in regulating store-operated Ca²⁺ influx in endothelial cells. We observed that the cell permeable CSD peptide inhibited thrombin-induced ER store Ca²⁺ release and store Ca²⁺ release-induced Ca²⁺ influx. CSD peptide also suppressed the thapsigargin-induced Ca²⁺

entry suggesting that CSD may directly interact with TRPC1 to regulate the Ca^{2+} influx via SOC. Further, we observed the specific binding of CSD to TRPC1 using the cell permeable AP-CSD peptide as well as ectopically expressed CSD sequence. Together, these findings suggest that the interaction between TRPC1 and CSD is crucial in regulating Ca^{2+} influx via SOC in endothelial cells.

Couet et al (1997) have recently identified CSD binding motif on $G_{i2\alpha}$ protein using phage display libraries. They showed that CSD sequence interacts with aromatic amino acid containing motifs: $\Phi X \Phi X X X X \Phi$ and $\Phi X X X X \Phi X X \Phi$, where Φ is an aromatic residue (Trp, Phe, or Tyr). We noted that the deduced amino acid sequence of TRPC1 had similar CSD binding motif in the C-terminus (FRTSKYAMF [$\Phi X X X X \Phi X X \Phi$]). Thus, we used CSD binding motif sequence present in the TRPC1 C-terminus (FRTSKYAMF, TRPC1-C9 peptide) to study its effects on Ca^{2+} influx via SOC. Incubation of HPAEC with AP-TRPC1-C9 peptide was shown to inhibit the store Ca^{2+} release-activated Ca^{2+} influx in HPAEC. We also observed specific binding of AP-TRPC1-C9 peptide to Cav-1 indicating that TRPC1 interaction with Cav-1 is required for Ca^{2+} influx via SOC.

Caveolae have been shown to form mobile signaling platforms by sequestering multiple signaling proteins that bind to CSD (Schlegel and Lisanti, 2001). Using Indo-1 and a confocal laser scanning system, Isshiki et al (1998) identified that Ca^{2+} waves preferentially occurred in the Cav-1-rich cell edges in response to shear stress or ATP in bovine aortic endothelial cells. They also demonstrated by engineering Ca^{2+} sensing yellow cameleon targeted to caveolae that Ca^{2+} influx in response to ER store depletion occurred preferentially in caveolae (Isshiki et al., 2002). Ca^{2+} influx in endothelial caveolae was markedly reduced by disturbing the caveolae structure with methyl- β -cyclodextrin (Bergdahl et al., 2003). Other studies have shown the

interaction between SOC (i.e., TRP channels) and IP₃-receptors (Boulay et al., 1999; Brownlow et al., 2004) and IP₃-receptors were associated with the caveolae signaling complex (Lockwich et al., 2000; Isshiki and Anderson, 2003). As we observed the inhibition of thrombin-induced ER store Ca²⁺ release by both cell permeable AP-CSD and AP-TRPC1-C9 peptides in HPAEC suggest that these peptides may be interfering in the assembly of signaling complex in the caveolae and thus may affect the ER associated IP₃-receptor function in endothelial cells.

Cav-1 is known to be abundantly expressed in endothelial cells (Minshall et al., 2000; Oh and Schnitzer, 2001), thus making it an important determinant of Ca²⁺ signaling in these cells. Overexpression of Cav-1 in endothelial cells was shown to impair caveolae-mediated signaling events in endothelial cells (Minshall et al., 2000). We have shown that *Src* family tyrosine kinase by promoting Tyr-14 phosphorylation of Cav-1 regulated a crucial function of caveolae in endothelial cells, caveolae-mediated endocytosis (Minshall et al., 2000, Shajahan et al., 2004; Tirupathi et al., 1997). In the present study, we observed that both basal and thrombin-induced Tyr-14 phosphorylation of Cav-1 were prevented by the cell permeable CSD peptide. CSD peptide concentration at 10 μM prevented thrombin-induced Tyr-14 phosphorylation on Cav-1, whereas this concentration had no significant effect on either ER store Ca²⁺ release or Ca²⁺ influx in HPAEC. This finding suggests that Tyr-14 phosphorylation on Cav-1 is apparently not required for Ca²⁺ influx via SOC. We also co-transfected Wt-Cav-1 or Cav-1-14F mutant with TRPC1 cDNA in an endothelial cell line (HMEC), and measured thrombin-induced increase in [Ca²⁺]_i. TRPC1 expression alone increased thrombin-induced increase in [Ca²⁺]_i; whereas co-expression of either Wt-Cav-1 or Cav-1-14F mutant with TRPC1 prevented the increase in [Ca²⁺]_i, indicating that Cav-1 binding to TRPC1 is more important in regulating SOC function in endothelial cells than Cav-1 phosphorylation on Tyr-14.

In summary, we showed that the cell permeable CSD peptide inhibited thrombin-induced ER store Ca^{2+} release and store Ca^{2+} release activated Ca^{2+} influx in human vascular endothelial cells. We identified the CSD docking sequence on TRPC1 C-terminal region as being crucial in regulating Ca^{2+} signaling via SOC in endothelial cells. In addition, we showed that binding of CSD peptide to key molecules is required for the activation of TRPC1-mediated Ca^{2+} signaling pathways. Thus, the interaction of CSD with TRPC1 plays an important role in the mechanism of store-operated Ca^{2+} influx, and thereby may regulate endothelial function.

References

- Bergdahl A, Gomez MF, Dreja K, Xu SZ, Adner M, Beech DJ, Broman J, Hellstrand P, and Sward K (2003). Cholesterol depletion impairs vascular reactivity to endothelin-1 by reducing store-operated Ca^{2+} entry dependent on TRPC1. **Circ Res.** 93:839-847.
- Bernatchez PN, Bauer PM, Yu J, Prendergast JS, He, P, and Sessa WC (2005) Dissecting the molecular control of endothelial NO synthase by caveolin-1 using cell-permeable peptides. **Proc Natl Acad Sci U S A.** 102:761-766.
- Birnbaumer L, Yidirim E, and Abramowitz J (2003). A comparison of the genes coding for canonical TRP channels and their M, V and P relatives. **Cell Calcium.** 33:419-432.
- Boulay G, Brown DM, Qin N, Jiang M, Dietrich A, Zhu MX, Chen Z, Birnbaumer M, Mikoshiba K, and Birnbaumer L (1999) Modulation of $\text{Ca}(2+)$ entry by polypeptides of the inositol 1,4, 5-trisphosphate receptor (IP3R) that bind transient receptor potential (TRP): evidence for roles of TRP and IP3R in store depletion-activated $\text{Ca}(2+)$ entry. **Proc Natl Acad Sci U S A.** 96:14955-14960.
- Brazer SC, Singh BB, Liu X, Swaim W, and Ambudkar IS (2003). Caveolin-1 contributes to assembly of store-operated Ca^{2+} influx channels by regulating plasma membrane localization of TRPC1. **J Biol Chem.** 278:27208-27215.
- Brough GH, WU S, Cioffi D, Moore TM, Li M, Dean N, and Stevens T (2001) Contribution of endogenously expressed Trp1 to a Ca^{2+} -selective, store-operated Ca^{2+} entry pathway. **FASEB J.** 15:1727-1738.
- Brownlow SL, Harper AGS, Harper MT, and Sage SO (2004). A role for hTRPC1 and lipid raft domains in store-mediated calcium entry in human platelets. **Cell Calcium.** 35:107-113.

- Bucci M, Gratton JP, Rudic RD, Acevedo L, Roviezzo F, Cirino G, and Sessa WC (2000) In vivo delivery of the caveolin-1 scaffolding domain inhibits nitric oxide synthesis and reduces inflammation. **Nat Med.** 6:1362-1367.
- Cool DR and Hardiman A (2004) C-Terminal sequencing of peptide hormones using carboxypeptidase Y and SELDI-TOF mass spectrometry. **Biotechniques.** 36:32-34.
- Couet J, Li S, Okamoto T, Ikezu T, and Lisanti MP (1997) Identification of peptide and protein ligands for the caveolin-scaffolding domain. Implications for the interaction of caveolin with caveolae-associated proteins. **J Biol Chem.** 272:6525-6533.
- del Pozo MA, Balasubramanian N, Alderson NB, Kiosses WB Grande-Garcia A, Anderson RGW, and Schwartz MA (2005) Phospho-caveolin-1 mediates integrin-regulated membrane domain internalization. **Nature Cell Biol.** 7:901-908.
- Dietrich A, Mederos Y, Schnitzler M, Emmel J, Kalwa H, Hofmann T, and Gudermann T (2003) N-linked protein glycosylation is a major determinant for basal TRPC3 and TRPC6 channel activity. **J Biol Chem.** 278:47842-47852.
- Drab M, Verkade P, Elger M, Kasper M, Lohn M, Lauterbach B, Menne J, Lindschau C, Mende F, Luft FC, Schedl A, Haller H, and Kurzchalia TV (2001) Loss of caveolae, vascular dysfunction, and pulmonary defects in caveolin-1 gene-disrupted mice. **Science.** 293:2449-2452.
- Ellis CA, Malik AB, Gilchrist A, Hamm H, Sandoval, Voyno-Yaseketskaya T, and Tirupathi C (1999) Thrombin induces proteinase-activated receptor-1 gene expression in endothelial cells via activation of Gi-linked ras/mitogen-activated protein kinase pathway. **J Biol Chem.** 274:13718-13727.
- Freichel M, Suh SH, Pfeifer A, Schweig U, Trost C, Weissgerber P, Biel M, Philipp S, Freise D, Droogmans G, Hofmann F, Flockerzi V, and Nilius B (2001) Lack of an endothelial store-

operated Ca^{2+} current impairs agonist-dependent vasorelaxation in TRP4^{-/-} mice. **Nat Cell Biol.** 3:121-127.

Groschner K, Hingel S, Lintschinger B, Balzer M, Romanin C, Zhu X, and Schreibmayer W (1998) Trp proteins form store-operated cation channels in human vascular endothelial cells. **FEBS Lett.** 437:101-106.

Hardiman A, Friedman TC, Grunwald Jr WC, Furuta M, Zhu Z, Steiner DF, and Cool DR (2005) Endocrinomic profile of neurointermediate lobe pituitary prohormone processing in PC1/3- and PC2-null mice using SELDI-TOF mass spectrometry. **J Mol Endocrinol.** 34:739-751.

Isshiki M and Anderson RGW (2003) Function of caveolae in Ca^{2+} entry and Ca^{2+} -dependent signal transduction. **Traffic.** 4:717-723.

Isshiki M, Ando J, Korenaga R, Kogo H, Fujimoto T, Fujita T, and Kamiya A (1998) Endothelial Ca^{2+} waves preferentially originate at specific loci in caveolin-rich cell edges. **Proc Natl Acad Sci U S A.** 95:5009-5014.

Isshiki M, Ying YS, Fujita T, and Anderson RGW (2002) A molecular sensor detects signal transduction from caveolae in living cells. **J Biol Chem.** 277:43389-43398.

Liu X, Wang W, Sing BB, Lockwich T, Jadlowiec J, O'Connell B, Wellner R, Zhu MX, and Ambudkar IS (2000) Trp1, a candidate protein for the store-operated Ca^{2+} influx mechanism in salivary gland cells. **J Biol Chem.** 275:3403-3411.

Lockwich TP, Liu X, Singh BB, Jadlowiec J, Weiland S, and Ambudkar IS (2000) Assembly of Trp1 in a signaling complex associated with caveolin-scaffolding lipid raft domains. **J Biol Chem.** 275:11934-11942.

Michel JB, Feron O, Sacks D, and Michel T (1997) Reciprocal regulation of endothelial nitric-oxide synthase by Ca^{2+} -calmodulin and caveolin. **J Biol Chem.** 272:15583-15586.

- Minshall RD, Tiruppathi C, Vogel SM, Niles WD, Gilchrist A, Hamm HE, and Malik AB (2000) Endothelial cell-surface gp60 activates vesicle formation and trafficking via G(i)-coupled Src kinase signaling pathway. **J Cell Biol.** 150:1057-1070.
- Montell C, Birnbaumer L, and Flockerzi V (2002) The TRP channels, a remarkably functional family. **Cell** 108:595-598.
- Nilius B and Droogmans G (2001) Ion Channels and Their Functional Role in Vascular Endothelium. **Physiol Rev.** 81:1415-1459.
- Oh P and Schnitzer JE (2001) Segregation of heterotrimeric G proteins in cell surface microdomains. G_q binds caveolin to concentrate in caveolae, whereas G_i and G_s target lipid rafts by default. **Mol Biol Cell.** 12:685-698.
- Paria BC, Malik AB, Kwiatek AM, Rahman A, May MJ, Ghosh S, Tiruppathi C (2003) Tumor necrosis factor- α induces nuclear factor- κ B-dependent TRPC1 expression in endothelial cells. **J Biol Chem.** 278:37195-37203.
- Paria PC, Vogel SM, Ahmmed GU, Alamgir S, Shroff J, Malik AB, and Tiruppathi C (2004) Tumor necrosis factor- α -induced TRPC1 expression amplifies store-operated Ca²⁺ influx and endothelial permeability. **Am J Physiol Lung Cell Mol Physiol.** 287:L1303-L1313.
- Paria BC, Bair AM, Xue J, Yu Y, Malik AB, and Tiruppathi C (2006) Ca²⁺ influx-induced by PAR-1 activates a feed-forward mechanism of TRPC1 expression via NF- κ B activation in endothelial cells. **J Biol Chem.** May 18; [Epub ahead of print]
- Putney JW, Jr (1999) TRP, inositol 1,4,5-triphosphate receptors, and capacitative calcium entry. **Proc Natl Acad Sci USA.** 96:14669-14671.
- Pedersen, S. F., Owsianik, G., and Nilius, B. (2005) TRP channels: An overview. **Cell Calcium.** 38, 233-252.

Sandoval R, Malik AB, Minshall RD, Kouklis P, Ellis CA, and Tiruppathi C (2001a) Ca^{2+} signaling and PKC α activate increased endothelial permeability by disassembly of VE-cadherin junctions. **J Physiol (Lond)** 533:433-335.

Sandoval R, Malik AB, Naqvi T, Mehta D, and Tiruppathi C (2001b) Requirement of Ca^{2+} signaling in the mechanism of thrombin-induced increase in endothelial permeability. **Am J Physiol Lung Cell Mol Physiol**. 280:L239-L247.

Schlegel A and Lisanti MP (2001) Caveolae and their coat proteins, the caveolins: from electron microscopic novelty to biological launching pad. **J Cell Physiol**. 186:329-337.

Shajahan AN, Sverdlov M, Hirth AM, Timblin BK, Tiruppathi C, Malik AB, and Minshall RD (2004) *Src*-dependent caveolin-1 phosphorylation destabilizes caveolin-1 oligomers and activates vesicle fission in endothelial cells. **Mol Biol Cell**.15:330a

Tiruppathi C, Freichel M, Vogel SM, Paria BC, Mehta D, Flockerzi V, and Malik AB (2002) Impairment of store-operated Ca^{2+} entry in TRPC4 $^{-/-}$ mice interferes with increase in lung microvascular permeability. **Circ Res**. 91:70-76.

Tiruppathi C, Minshall RD, Paria BC, Vogel SM, and Malik AB (2003) Role of Ca^{2+} signaling in the regulation of endothelial permeability. **Vascul Pharmacol**. 39:173-185.

Tiruppathi C, Song W, Bergenfeldt M, Sass P, Malik AB (1997) Gp60 activation mediates albumin transcytosis in endothelial cells by tyrosine kinase-dependent pathway. **J Biol Chem**. 272:25968-25975.

Zhu L, Schwegler-Berry D, Castranova V, and He P (2004) Internalization of caveolin-1 scaffolding domain facilitated by Antennapedia homeodomain attenuates PAF-induced increase in microvessel permeability. **Am J Physiol Heart Circ Physiol**. 286:H195-H201.

MOL #21741

Footnotes: This work was supported by NIH grants GM58531, P01 HL077806, and
T32HL007829

Figure Legends:

Fig. 1A: Internalization of AP or AP-CSD peptide in HPAEC. HPAEC grown to confluence on glass coverslips were washed and incubated with 1% FBS medium containing either AP (25 μ M) or AP-CSD (25 μ M) for 4 h at 37^oC. After incubation, cells were washed 3X on ice with acid buffer (50 mM acetate buffer pH 4.5 containing 0.5 M NaCl) to remove cell surface bound peptides, fixed with 2% PFA, and permeabilized with 0.1% Triton X-100 (Bucci et al., 2000). Cells were then stained with rhodamine labeled streptavidin and images were obtained from Zeiss Axiovert 25 fluorescent microscope.

Fig. 1B: SELDI-TOF mass spectrometric analysis of peptides associated with HPAEC. HPAEC were incubated with either CSD (AP-CSD) or AP peptides for 4 h at 37^oC. After this incubation, cell pellets obtained were used for SELDI-TOF mass spectrometric analysis as described in **Methods**. The molecular mass of CSD (4972.57 daltons) and AP (2473.49 daltons) were identified using the synthetic peptides. A representative analysis is shown in this figure. Control, cells not exposed to either CSD or AP peptide; CSD-50, cells incubated with 50 μ M CSD; CSD-100, cells incubated with 100 μ M CSD; AP-50, cells incubated with 50 μ M AP; AP-100, cells incubated with 100 μ M AP; M/Z indicates mass/charge and is represented as daltons in the spectra. The relative concentrations of peptides present inside the cells were calculated using spectra from different concentrations of peptides as described in **Methods**. The experiment was repeated three times and the results are summarized in **Table 1**.

Fig. 1C: (*upper panel*) CSD peptide inhibits thrombin-induced increase in intracellular Ca²⁺ in HPAEC. HPAEC grown to confluence were incubated with the indicated concentrations of AP-CSD peptide and then used for measuring cytosolic Ca²⁺ (see details in **Methods**). Cells were stimulated with thrombin in the presence of nominal Ca²⁺ (1.26 mM) in the extracellular

medium. Arrow indicates the time at which cells were stimulated with thrombin (50 nM). Results shown are representative of four experiments. In each experiment, 30 to 50 cells were selected to measure change in $[Ca^{2+}]_i$. The relative area of peak increase in $[Ca^{2+}]_i$ after thrombin-stimulation in control and AP-CSD peptide exposed cells were compared (*lower panel*). * = $p < 0.01$; ** = $p < 0.005$. In D (*upper panel*), the experiment was carried out as described in C, except that cells were incubated with AP peptide. Results shown are representative of four experiments. The relative area of peak increase in $[Ca^{2+}]_i$ after thrombin-stimulation in control and AP peptide exposed cells were compared (*lower panel*).

Fig. 2A: AP-CSD peptide inhibits thrombin-induced ER store Ca^{2+} release and Ca^{2+} release-induced Ca^{2+} influx in HPAEC. HPAEC incubated with indicated concentrations of AP-CSD peptide were used for measuring ER store Ca^{2+} release and Ca^{2+} release-induced Ca^{2+} influx. After fura-2/AM loading, cells were washed 2X, placed in Ca^{2+} - and Mg^{2+} -free HBSS, and then stimulated with thrombin (50 nM). After return to base-line levels, 1.5 mM $CaCl_2$ was added to the extracellular medium to induce Ca^{2+} influx. *Arrows*, times at which thrombin (T) or Ca^{2+} was added. In **B**, relative areas of initial ER store Ca^{2+} release and the Ca^{2+} influx peaks were compared with control and peptide-treated groups. * = $p < 0.01$; ** < 0.005.

Fig. 2C: CSD peptide inhibits thapsigargin (Thap)-induced increase in $[Ca^{2+}]_i$ in HPAEC. HPAEC incubated with the indicated concentrations of AP-CSD or AP peptides were used for measuring Thap-induced increase in $[Ca^{2+}]_i$ as described in **Methods**. Cells were placed in nominal Ca^{2+} (1.26 mM)-containing medium and then stimulated with thapsigargin (1 μ M). Arrow indicates the time at which thapsigargin was added. Results shown are representative of four experiments.

Fig. 3A: CSD interacts with TRPC1 in endothelial cells. HPAEC incubated with 50 μ M AP-CSD or AP peptide for 4 h at 37^oC were washed 3X with acid buffer (50 mM acetate buffer pH 5.0 containing 0.5 M NaCl) at 4^oC. Cells were lysed and CSD binding proteins were separated using streptavidin-agarose beads pull-down (see details in **Method**). The proteins associated with beads were separated on SDS-PAGE and immunoblotted with anti-TRPC1 antibody. The results shown are from representative experiments. The experiment was repeated 3 times, and the results obtained were similar. Lane 1, control; lane 2, AP peptide incubated cells; lane 3, AP-CSD peptide incubated cells; lane 4, cell lysate. IB, immunoblot.

Fig. 3B: Endogenous TRPC1 binds to ectopically expressed CSD domain in endothelial cells. HA-tagged-CSD sequence expressing plasmid was transfected into HMEC (see details in **Methods**). At 48 h after transfection, cell lysates were immunoprecipitated with anti-HA-monoclonal antibody (mAb). The precipitated proteins were separated on SDS-PAGE and immunoblotted with anti-TRPC1 polyclonal antibody (pAb). Lane 1, control; lane 2, vector transfected control; lane 3, HA-tagged-CSD sequence expressing plasmid transfected. Anti-TRPC1 Ab reacted (85 kDa) with HA-tagged-CSD sequence expressing cells. Cell lysates (50 μ g protein) from control, vector transfected, and HA-tagged CSD transfected were immunoblotted with anti-TRPC1 Ab to indicate that TRPC1 expression was not altered in HMEC (lower panel). IP, immunoprecipitate; IB, immunoblot.

Fig. 4: Cav-1 interacts with C-terminus of TRPC1. **A.** CSD binding consensus sequence in the C-terminus of TRPC1. **B.** HPAEC were incubated with 25 μ M concentration of either biotin labeled-AP peptide or biotin labeled AP-TRPC1 C-terminal peptide (residues 781-789 [AP-TRPC1-C9]) at 4 h at 37^oC in 1% FBS containing medium. After incubation, cell lysates were used for streptavidin-agarose pull-down (see details in **Methods**). Proteins associated with

streptavidin-agarose beads were separated on SDS-PAGE and immunoblotted with anti-Cav-1 antibody (top panel). Lane 1, control; lane 2, AP peptide treated cells; lane 3, AP-TRPC1-C9 peptide treated cells. Cell lysates (20 μg protein) from control, AP peptide, and AP-TRPC1-C9 peptide treated were immunoblotted with anti-Cav-1 Ab (lower panel).

Fig. 4 C and D: TRPC1 C-terminal synthetic peptide inhibits thrombin-induced increase in $[\text{Ca}^{2+}]_i$ in HPAEC. In **C**, HPAEC grown to confluence were incubated with the indicated concentrations of AP-TRPC1-C9 peptide (see details in **Methods**). After incubation, cells were used for measuring thrombin-induced increase in $[\text{Ca}^{2+}]_i$ described in **Fig. 1C**. Arrow indicates the time at which cells were stimulated with thrombin (50 nM). Results shown are representative of four experiments. In **D**, relative area of peak increase in $[\text{Ca}^{2+}]_i$ after thrombin-stimulation in control and AP-TRPC1-C9 peptide treated groups were compared. * $p < 0.01$.

Fig. 4 E and F: TRPC1 C-terminal synthetic peptide inhibits Ca^{2+} influx via TRPC1 in HPAEC. The experiment was carried out as described above in **Fig. 2A**. In **E**, after fura-2/AM loading, cells were washed 2X, placed in Ca^{2+} - and Mg^{2+} -free HBSS, and stimulated with thrombin (50 nM). After return to base-line levels, 1.5 mM CaCl_2 was added to the extracellular medium to induce Ca^{2+} influx. *Arrows*, times at which thrombin (T) or Ca^{2+} was added. Results shown are representative of four experiments. In **F**, relative area of initial ER store Ca^{2+} release and the Ca^{2+} influx peaks were compared with the control and the AP-TRPC1-C9 peptide treated cells. * $= p < 0.01$; ** $= p < 0.005$.

Fig. 5A: Cav-1 scaffolding sequence interacts with *Src* in HPAEC. HPAEC grown to confluence on culture dishes were incubated with either AP peptide or AP-CSD peptide in 1% FBS containing medium for 4 h at 37°C . After this incubation period, cells were washed, lysed, and lysates were used for streptavidin-agarose beads pull-down (see details in **Methods**).

Proteins associated with streptavidin-agarose beads were separated on SDS-PAGE, and immunoblotted with anti-*Src* mAb. The results shown are from representative experiments. The experiment was repeated 3 times, and the results obtained were similar. Cell lysates (50 μ g protein) from control, AP peptide, and AP-CSD peptide treated were immunoblotted with anti-*Src* mAb (lower panel).

Fig. 5B: CSD peptide inhibits Cav-1 phosphorylation on Tyr-14 in endothelial cells. HPAEC grown to confluence on culture dishes were incubated with either AP peptide or AP-CSD peptide (see details in **Methods**). After incubation, cells were washed and incubated in serum free medium for 2 h, and cells were stimulated with thrombin (50 nM) for the indicated times. After thrombin treatment, cells were placed on ice, washed 3X at 4^oC, lysed, the lysate proteins were separated on SDS-PAGE, and *Src* activation-dependent Cav-1 phosphorylation was detected by immunoblotting with anti-phospho-Tyr-14 cav-1 antibody. The results shown are from representative experiments. The experiment was repeated 3 times, and the results obtained were similar.

Fig. 5 C, D, and E: Cav-1 co-expression with TRPC1 prevents Ca²⁺ influx via SOC in endothelial cells. HMEC grown to 60 to 70% confluence were transfected with Myc-TRPC1 expression plasmid (1 μ g/ml) alone or co-transfected with either WT-Cav-1 (1 μ g/ml) or Cav-1-14F mutant (1 μ g/ml) expression constructs using LipofectAMINE Plus reagents (Ellis et al., 1999). In **C**, after transfection, cell were lysed and immunoblotted with either anti-Myc-mAb (to determine TRPC1 expression) or anti-Cav-1 Ab. In **D**, at 48 h after transfection cells were used for measuring cytosolic Ca²⁺ (see details in **Methods**). After fura-2 loading, cells were placed in nominal Ca²⁺ (1.26 mM)-containing medium and then stimulated with thrombin (50 nM). Arrow indicates the time at which thrombin (T) was added. Results shown are representative of four

MOL #21741

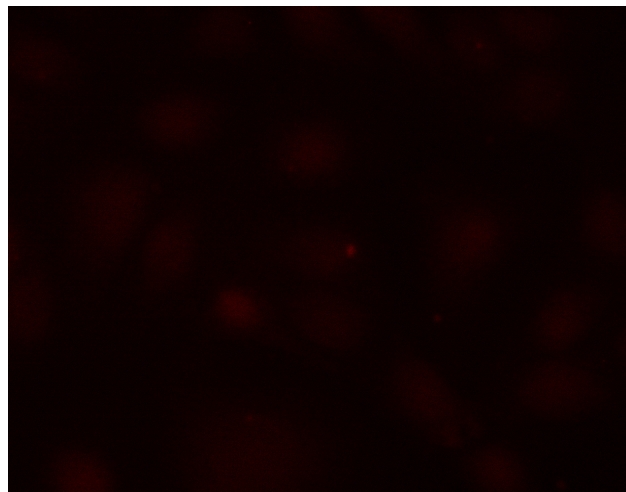
experiments. In **E**, the relative area of peak increase in $[Ca^{2+}]_i$ after thrombin-stimulation in control (vector transfected) and transfected cells were compared. ** = $p < 0.005$.

Table 1. Quantification of cell permeable peptides inside HPAEC

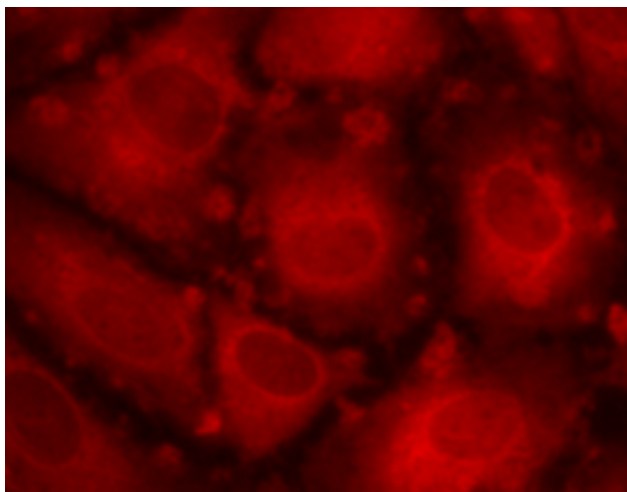
Peptide	Incubation Medium Concentration (μM)	Relative Peptide Concentration inside the cells (μM)
AP	0	ND
AP	50	25
AP	100	80
AP-CSD	0	ND
AP-CSD	50	20
AP-CSD	100	65

Cell volume was determined by incubating HPAEC with ^3H -mannitol as described in **Methods**. A volume of $2.5 \mu\text{l}/10^6$ cells was obtained. Cells were incubated with medium containing the indicated concentrations of peptides in a total volume of $2.46 \text{ ml}/10^6$ cells. The relative concentrations of peptides present in the cell extracts were calculated utilizing mass spectra from known peptide concentrations and cell volume (see details in **Methods**). Values reported are mean of three separate experiments. ND, not detectable.

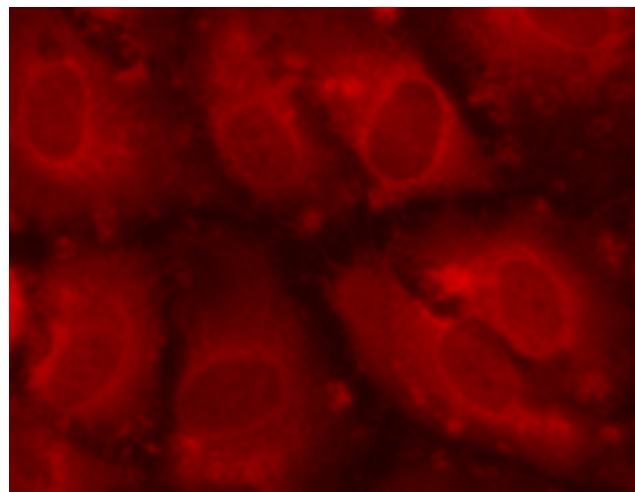
Fig. 1A



Rhodamine-Streptavidin



Biotin-AP-CSD



Biotin-AP

Fig. 1B

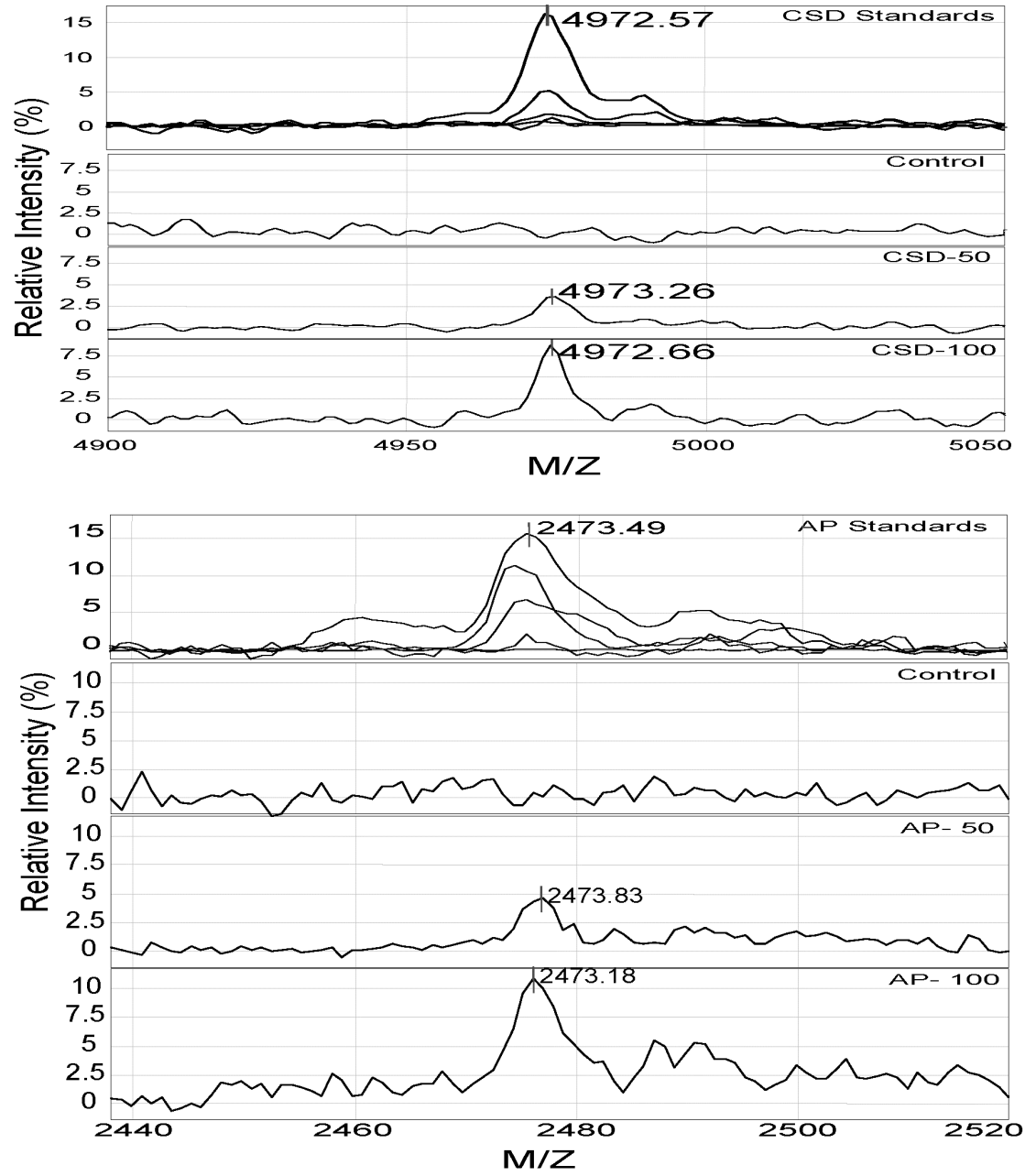


Fig. 1C

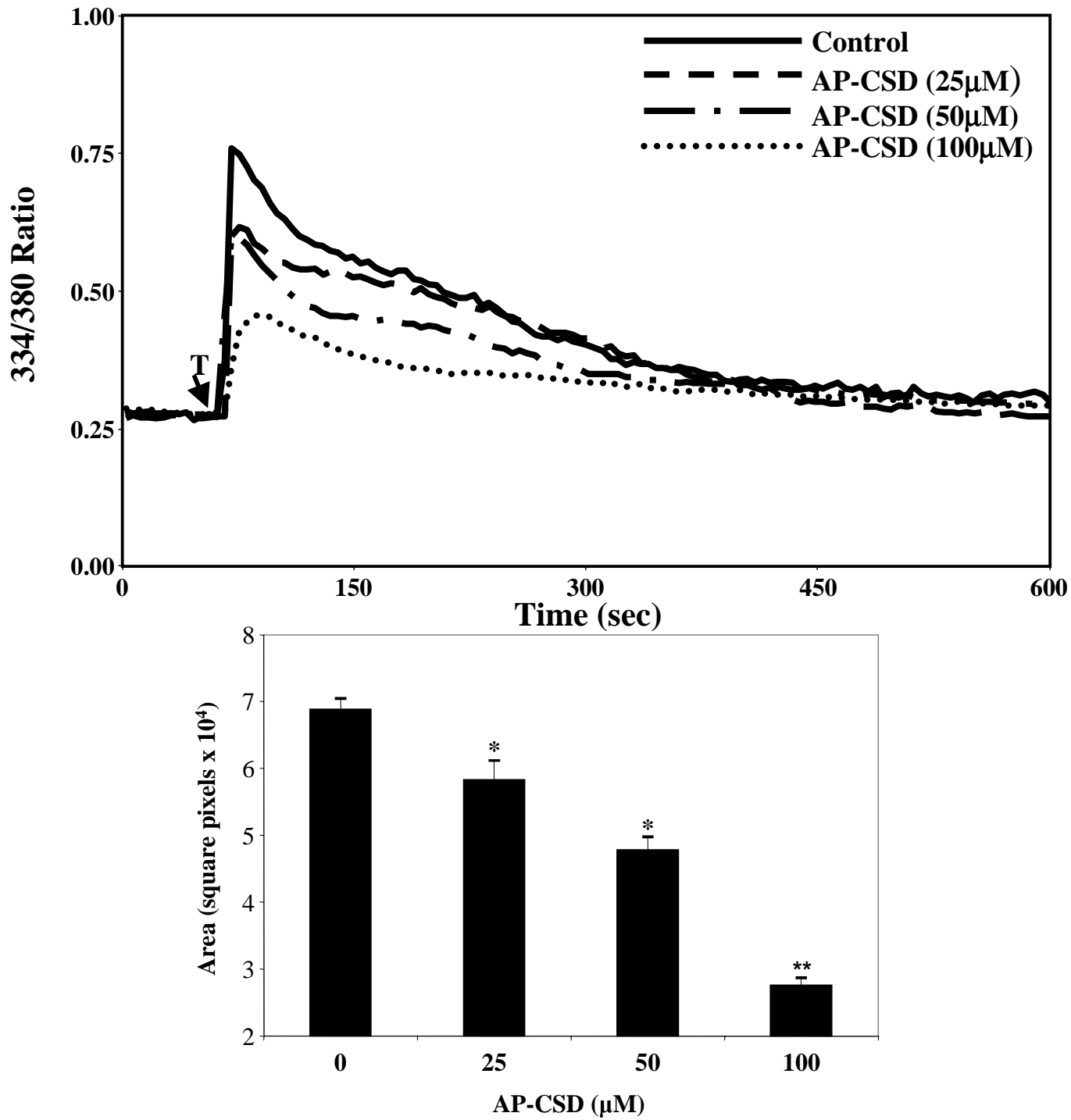


Fig. 1D

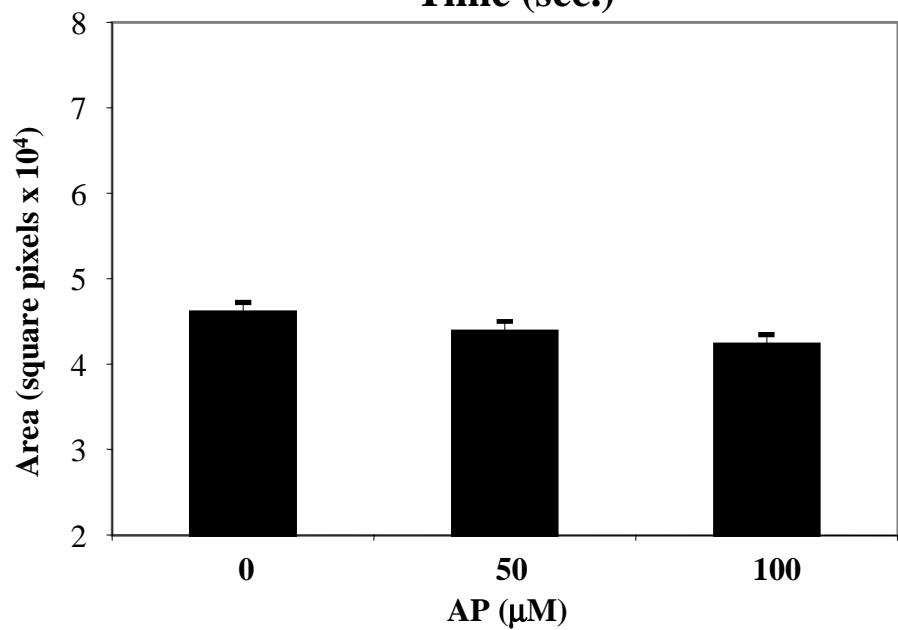
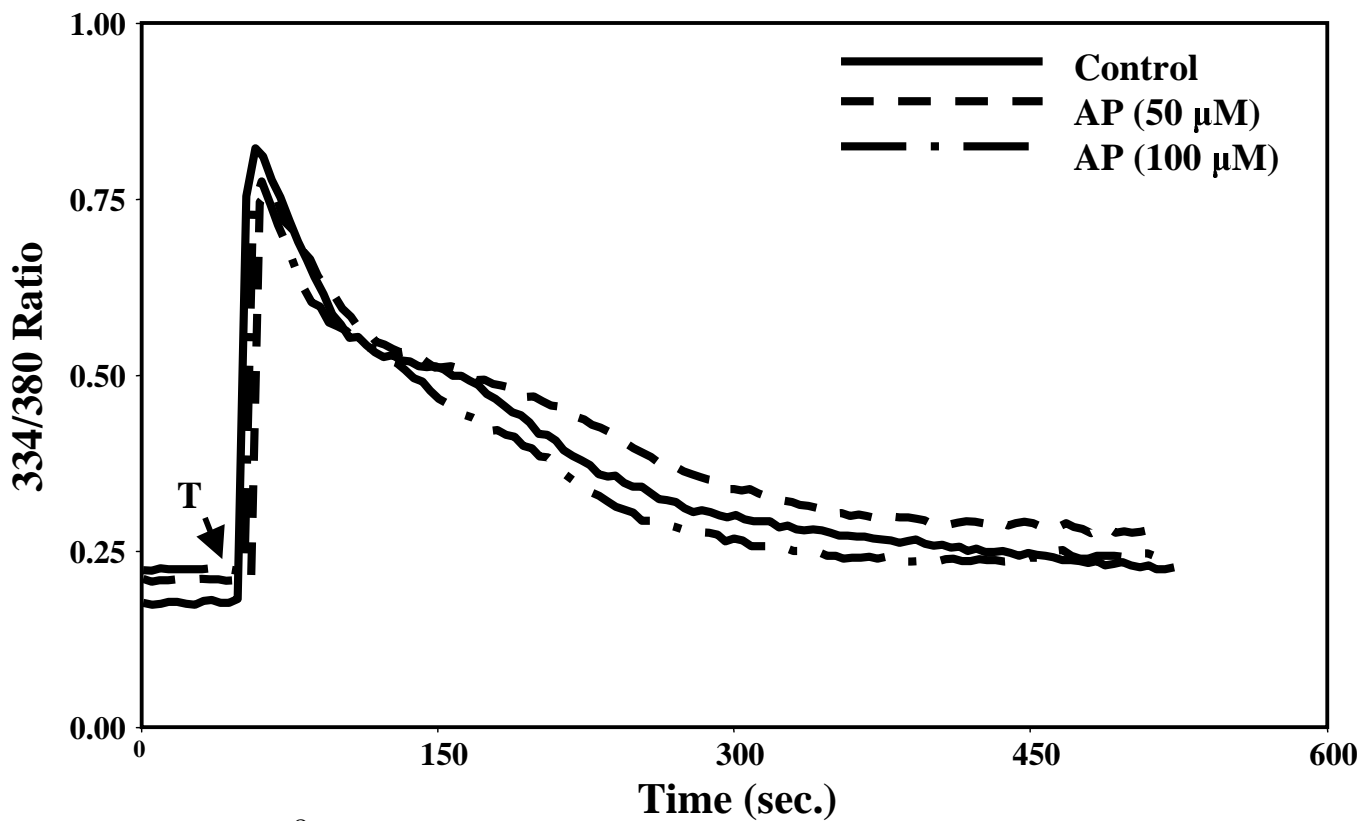


Fig. 2A

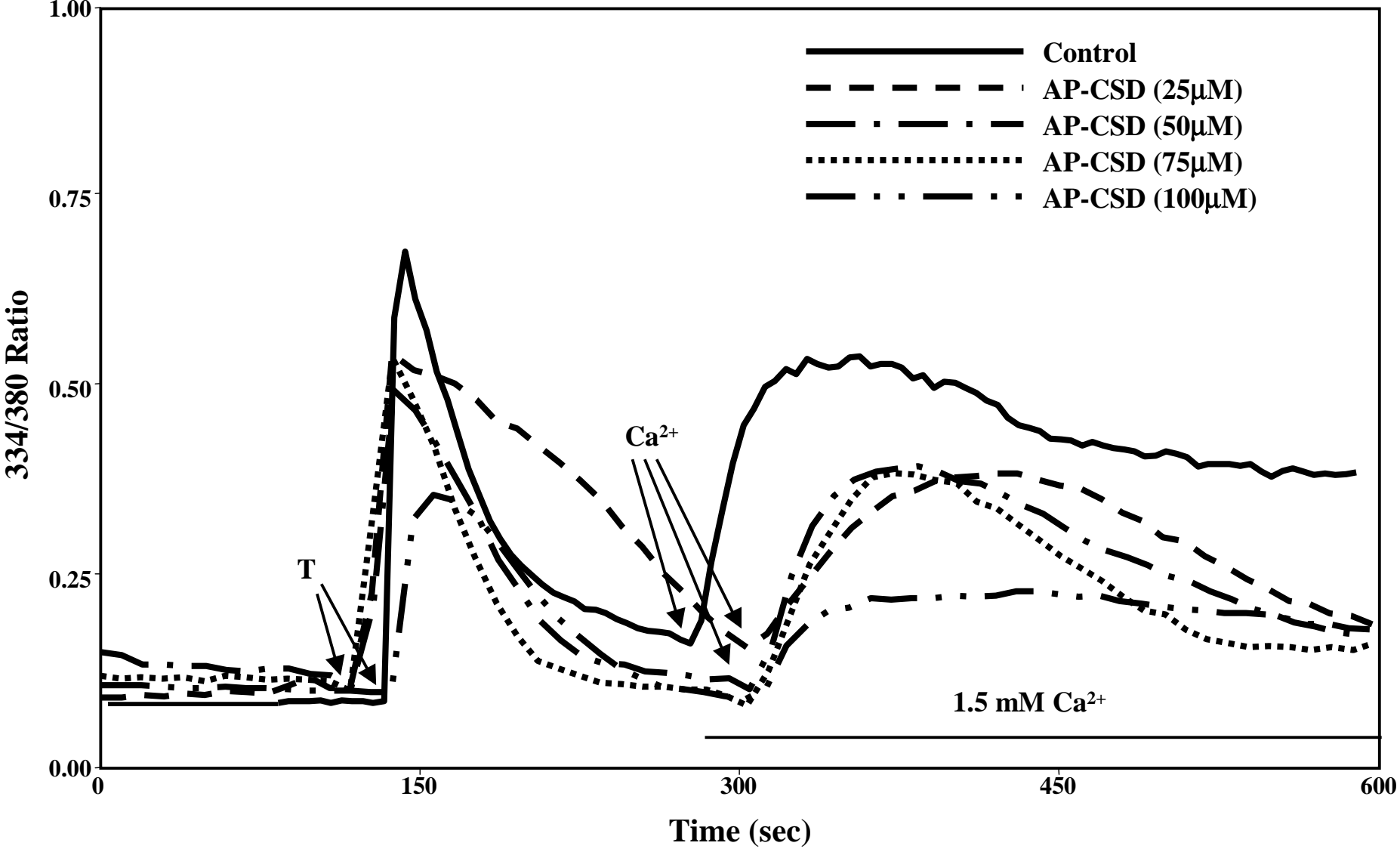


Fig. 2B

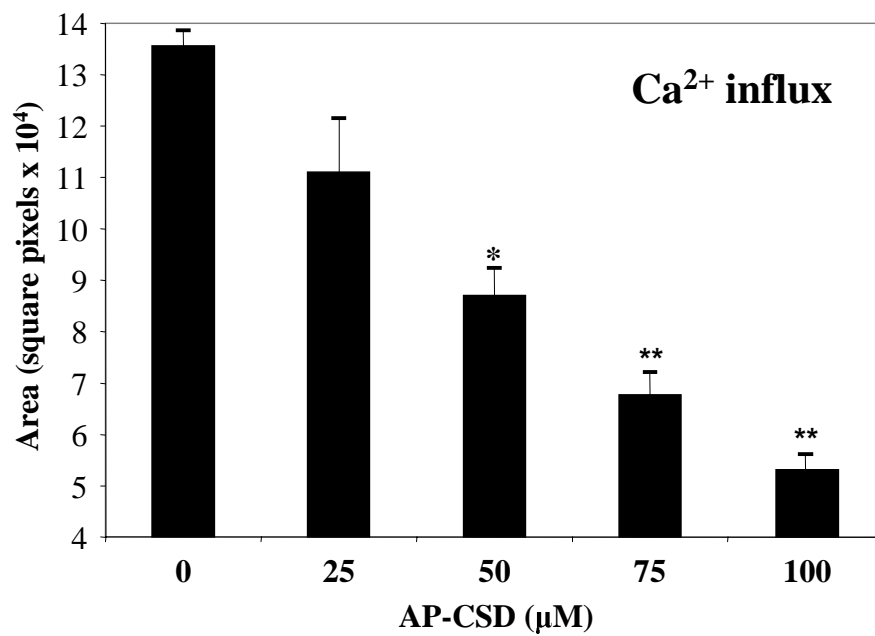
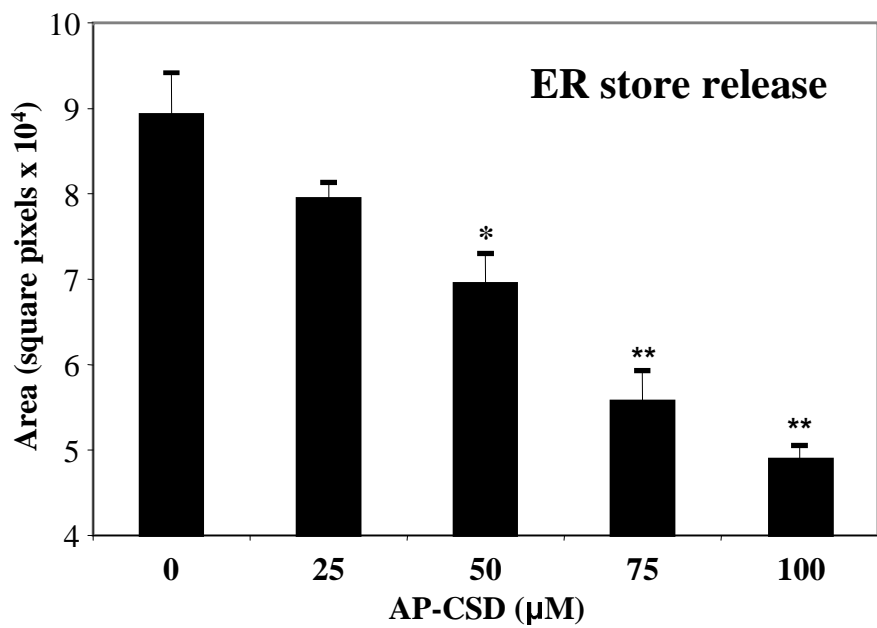


Fig. 2C

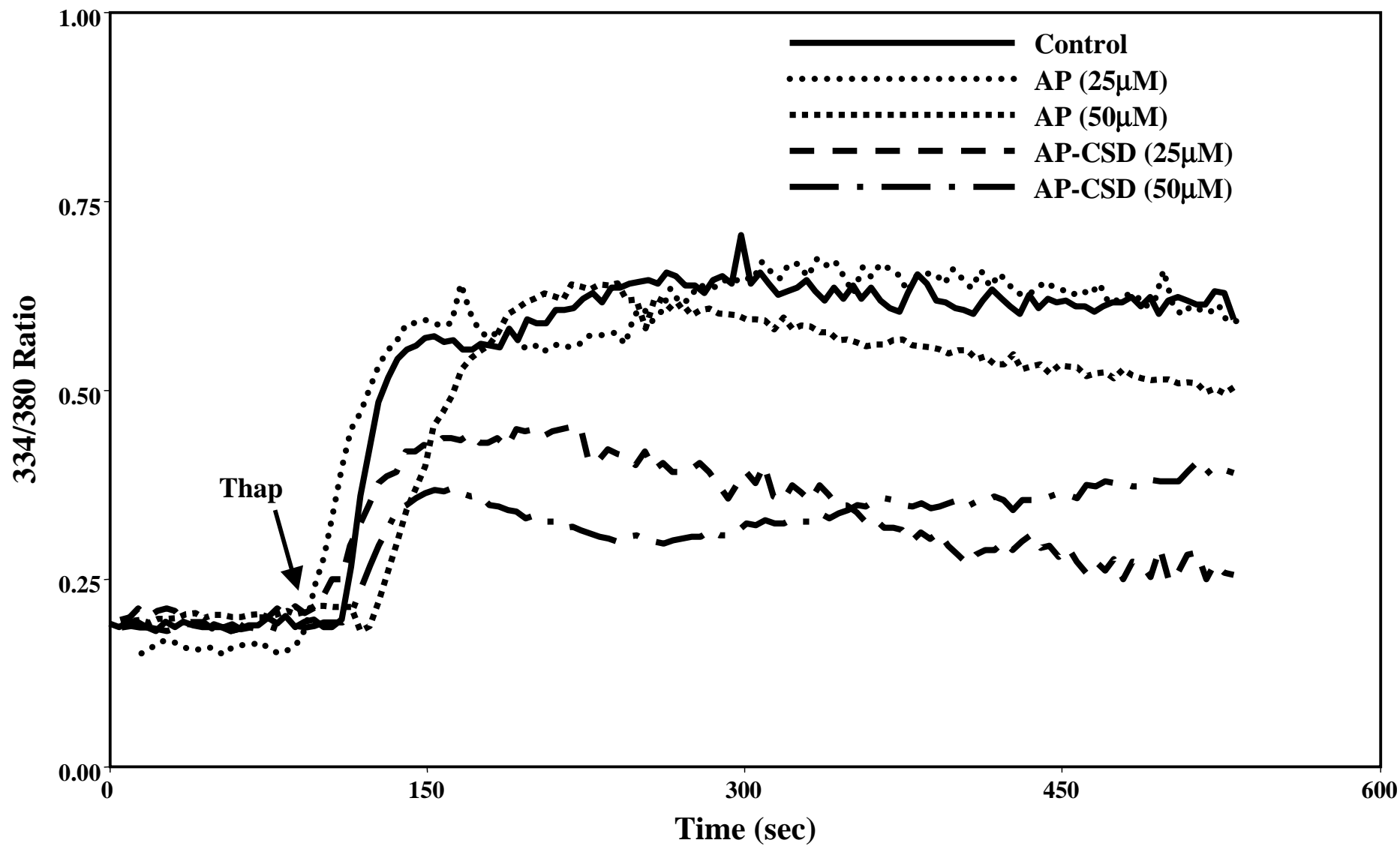


Fig. 3

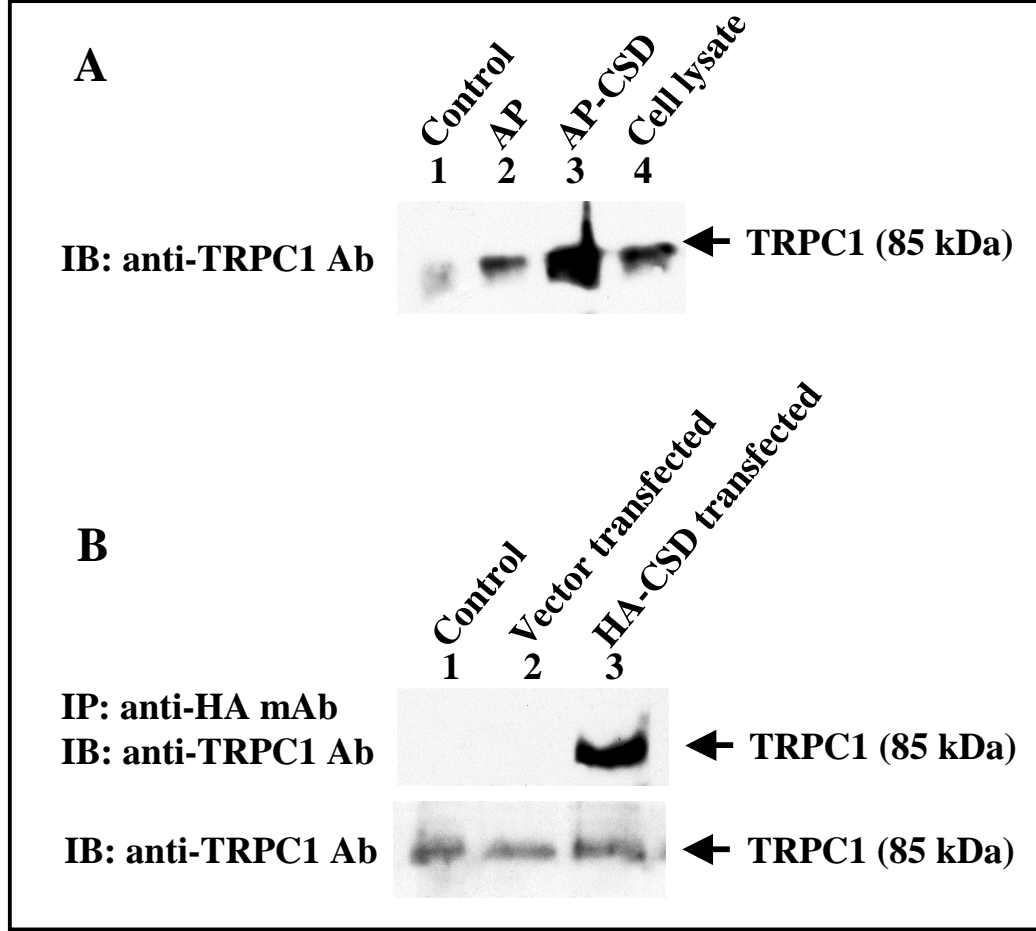


Fig. 4

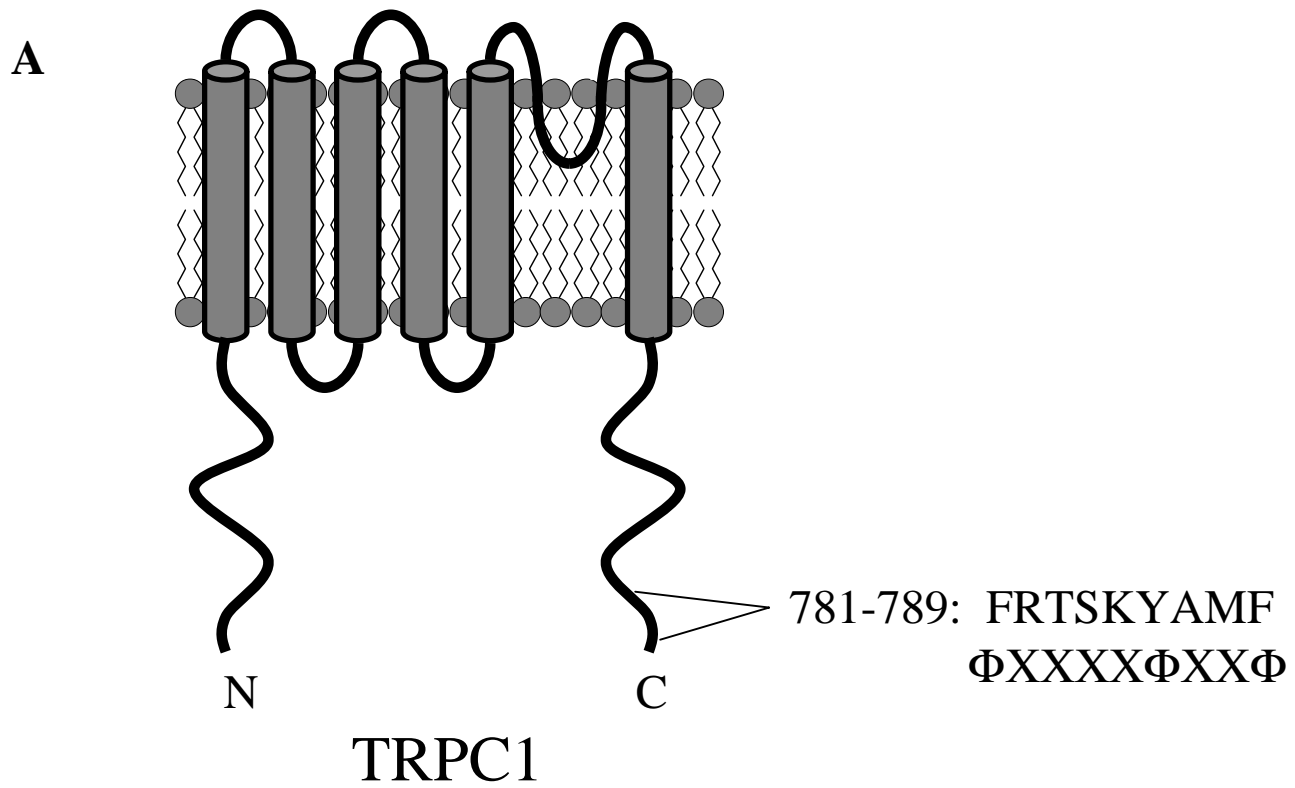


Fig. 4

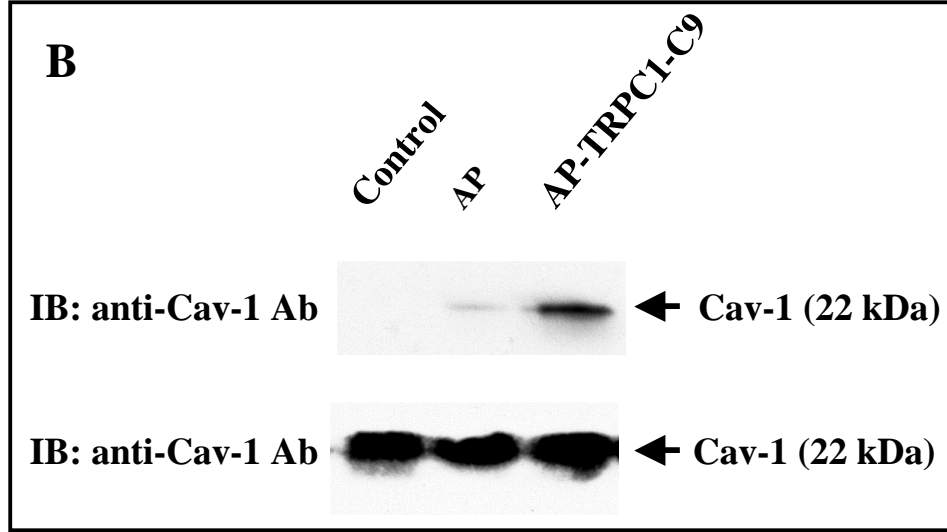


Fig. 4C

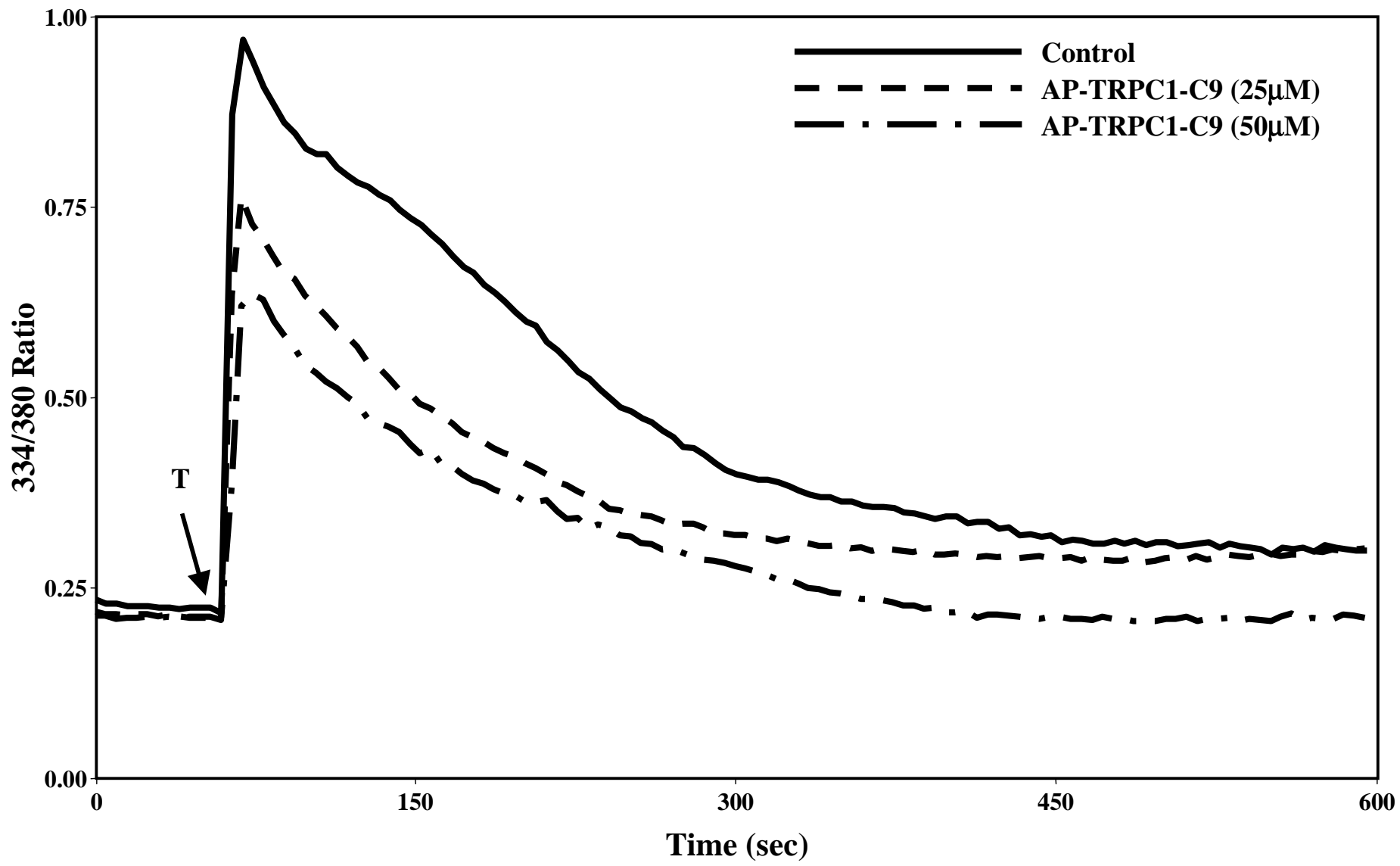


Fig. 4D

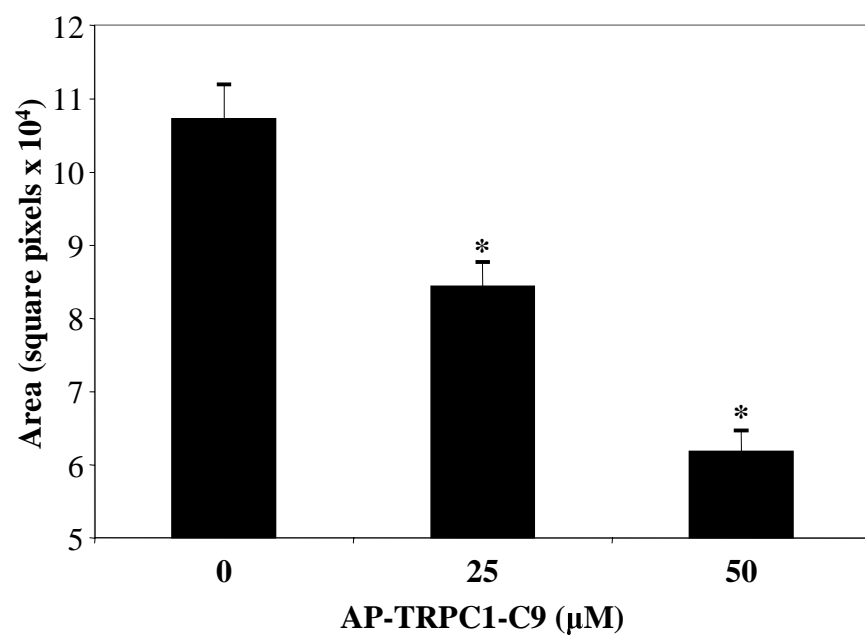


Fig. 4E

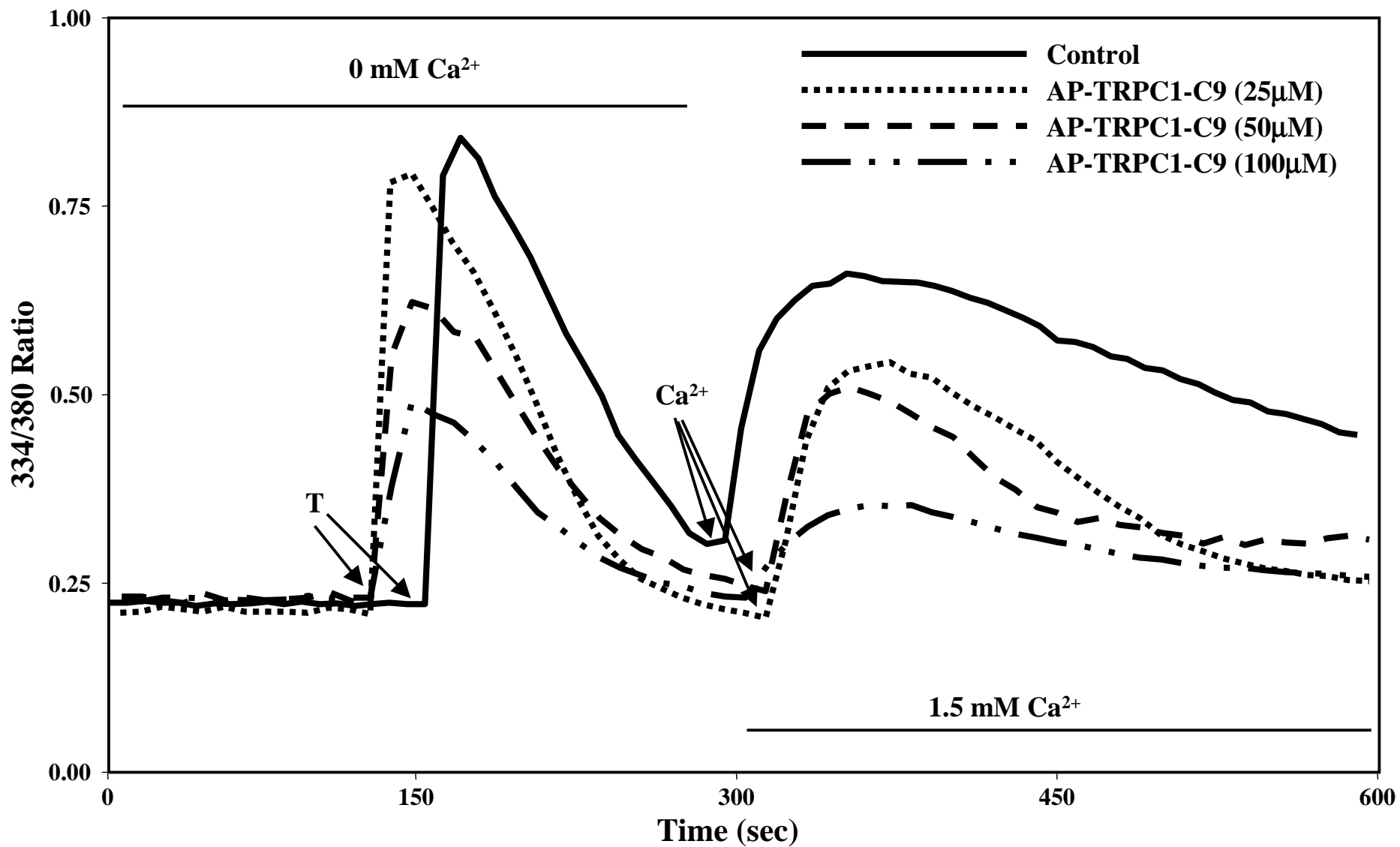


Fig. 4F

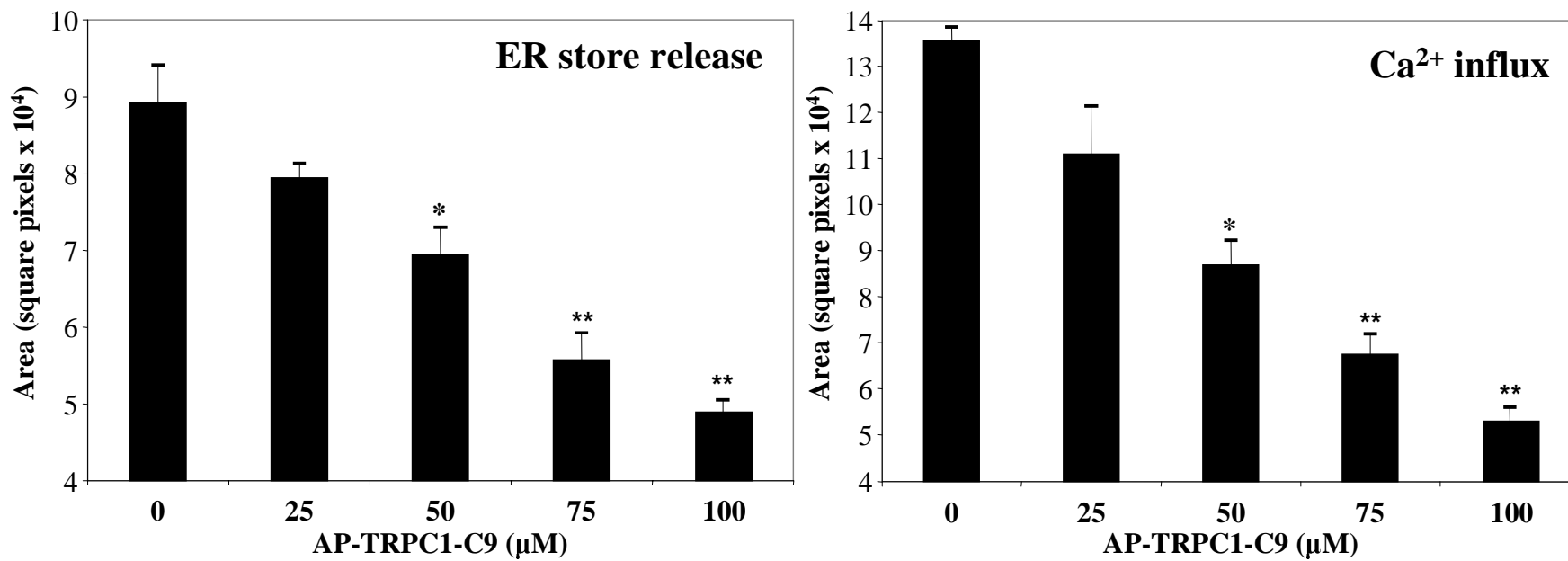


Fig. 5

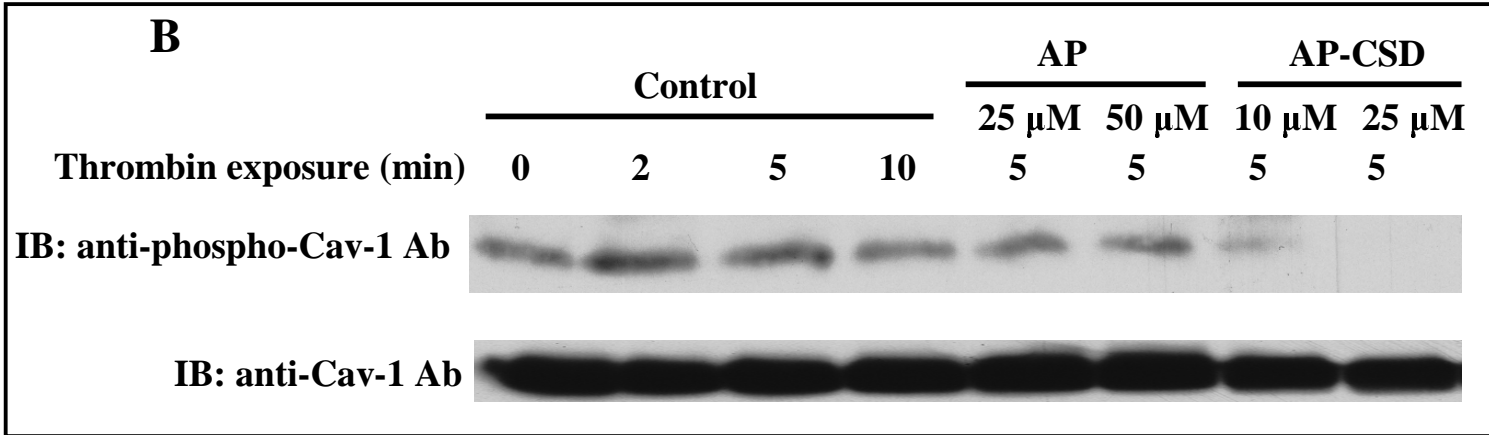
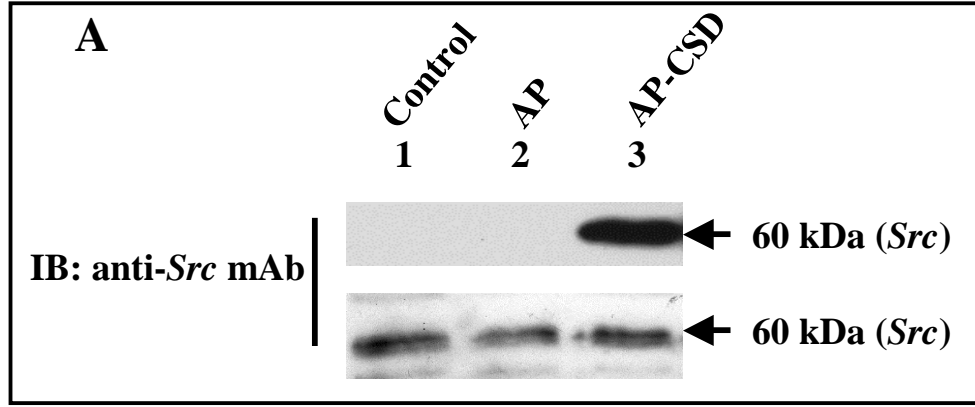


Fig. 5

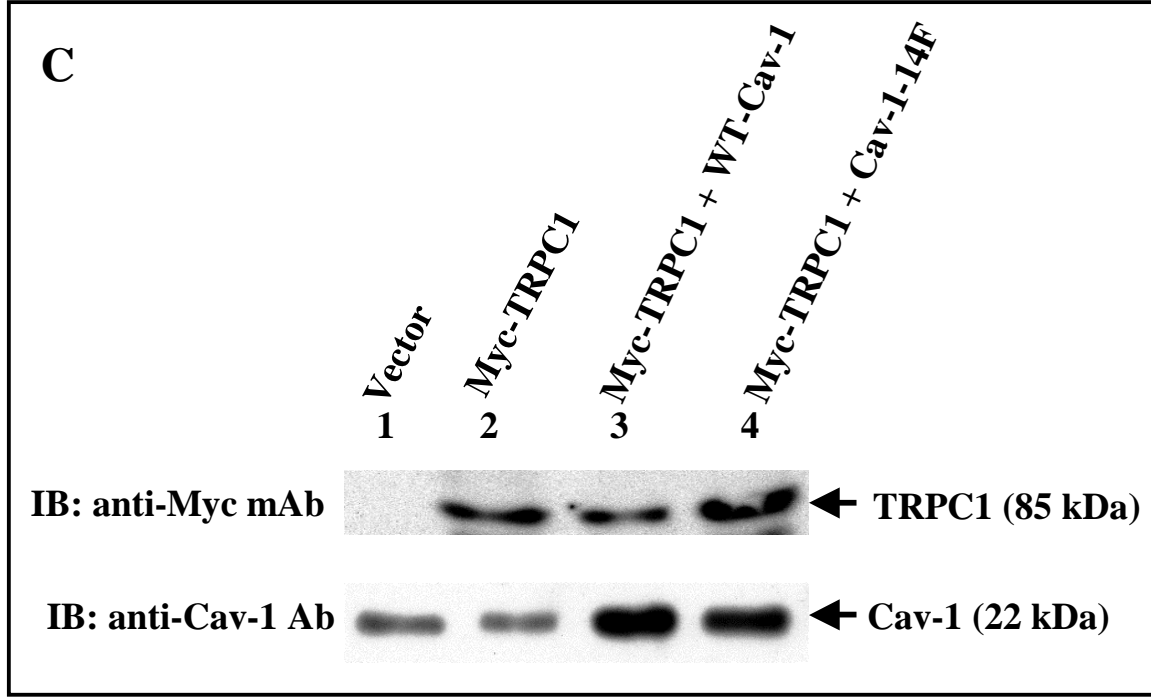


Fig. 5D

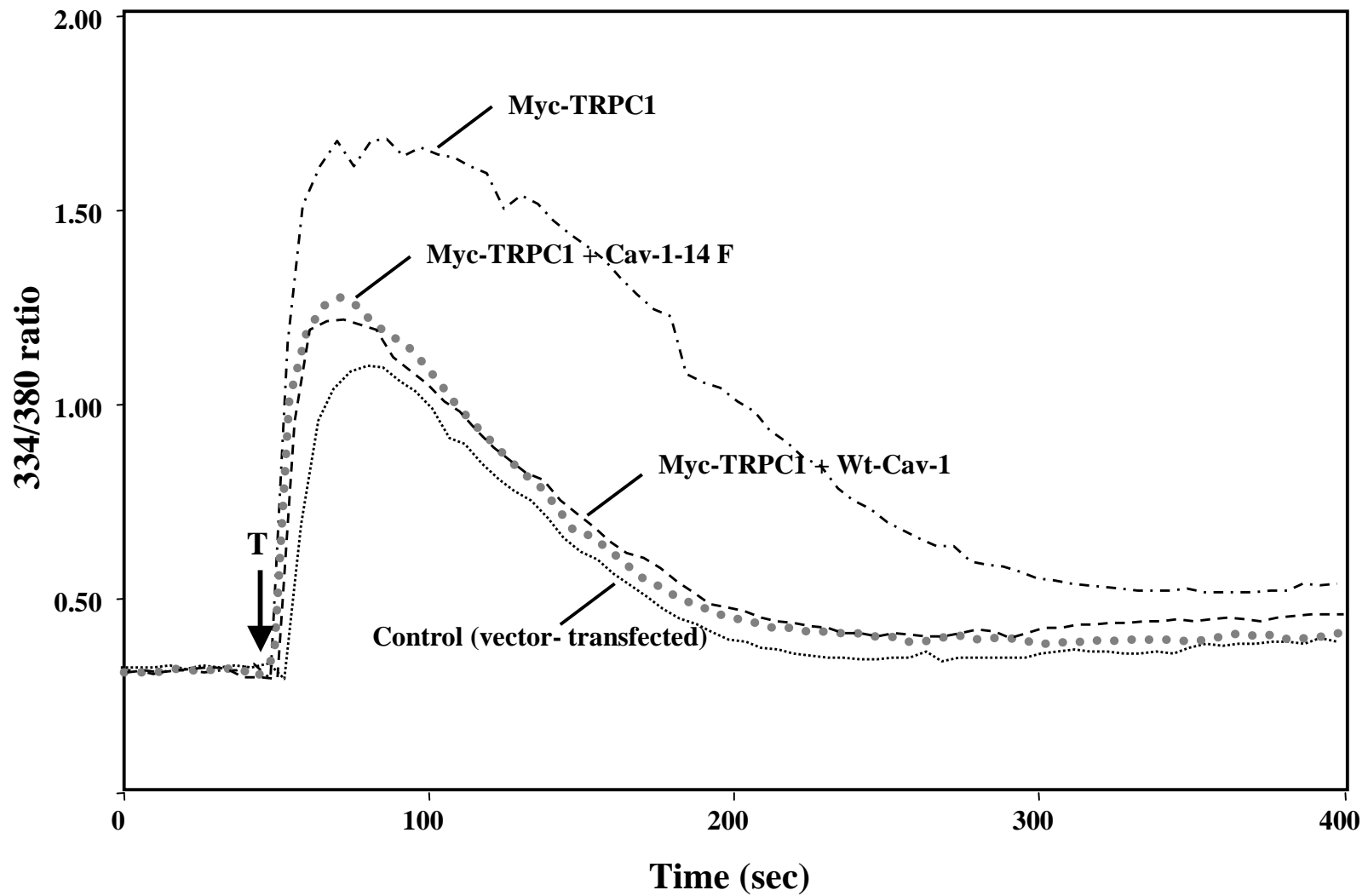


Fig. 5E

